PCCP

PAPER

View Article Online
View Journal | View Issue

Cite this: *Phys. Chem. Chem. Phys.*, 2016, **18**, 21976

High resolution GHz and THz (FTIR) spectroscopy and theory of parity violation and tunneling for 1,2-dithiine ($C_4H_4S_2$) as a candidate for measuring the parity violating energy difference between enantiomers of chiral molecules†

S. Albert,[ab] I. Bolotova,[a] Z. Chen,[a] C. Fábri,[a] L'. Horný,[a] M. Quack,*[a] G. Seyfang[a] and D. Zindel[a]

We report high resolution spectroscopic results of 1,2-dithiine-(1,2-dithia-3,5-cyclohexadiene, $C_4H_4S_2$) in the gigahertz and terahertz spectroscopic ranges and exploratory theoretical calculations of parity violation and tunneling processes in view of a possible experimental determination of the parity violating energy difference $\Delta_{pv}E$ in this chiral molecule. Theory predicts that the parity violating energy difference between the enantiomers in their ground state ($\Delta_{pv}E \simeq 1.1 \times 10^{-11}(hc)$ cm^{-1}) is in principle measurable as it is much larger than the calculated tunneling splitting for the symmetrical potential $\Delta E_{\pm} < 10^{-24}$ (hc) cm^{-1}. With a planar transition state for stereomutation at about 2500 cm^{-1} tunneling splitting becomes appreciable above 2300 cm^{-1}. This makes levels of well-defined parity accessible to parity selection by the available powerful infrared lasers and thus useful for one of the existing experimental approaches towards molecular parity violation. The new GHz spectroscopy leads to greatly improved ground state rotational parameters for 1,2-dithiine. These are used as starting points for the first successful analyses of high resolution interferometric Fourier transform infrared (FTIR, THz) spectra of the fundamentals ν_{17} (1308.873 cm^{-1} or 39.23903 THz), ν_{22} (623.094 cm^{-1} or 18.67989 THz) and ν_3 (1544.900 cm^{-1} or 46.314937 THz) for which highly accurate spectroscopic parameters are reported. The results are discussed in relation to current efforts to measure $\Delta_{pv}E$.

Received 3rd March 2016,
Accepted 1st June 2016

DOI: 10.1039/c6cp01493c

www.rsc.org/pccp

1 Introduction

According to the traditional point of view both in the framework of classical molecular structure[1–6] and within the ordinary quantum theory of molecules retaining only the electromagnetic force[7,8] the ground states of the enantiomers of chiral molecules are energetically exactly equivalent by symmetry.[1,5–10] This would result in a reaction enthalpy $\Delta_R H_0^{\ominus} = 0$ exactly for the stereomutation reaction (1). However, the situation has fundamentally changed with the discovery of parity violation.[11–21] In this case one predicts a small "parity violating" energy difference $\Delta_{pv}E_0$ between the ground states of the two enantiomers, leading to the prediction of a non-zero parity violating reaction enthalpy $\Delta_{pv}H_0^{\ominus}$:

$$\mathrm{P} \rightleftharpoons \mathrm{M} \quad \Delta_{pv}H_0^{\ominus} = N_A\Delta_{pv}E_0 \qquad (1)$$

where N_A is the Avogadro constant and we use the P and M notation for "axially chiral" molecules. This has important consequences for our understanding of the foundation of stereochemistry[10] and possibly also of the evolution of biomolecular homochirality.[22–29] There has been considerable theoretical work predicting the magnitude of $\Delta_{pv}E$, first qualitatively,[23,30] then in semiquantitative computations[31,32] all leading to exceedingly small absolute values. Recent progress in the theory of molecular parity violation, starting with our finding[33] that the early estimates of $\Delta_{pv}E$ were too low by up to two orders of magnitude for benchmark molecules such as H_2O_2 and related ones, confirmed by extensive subsequent work,[34–46] led to a new impetus to the field reviewed in ref. 9, 47 and 48, including serious attempts to detect parity violation in chiral molecules, so far unsuccessful, however. While several different experimental schemes concerning molecular parity violation have been proposed in the past[26,30,49–53] (see also the reviews in ref. 9, 10, 29, 47 and 54–56), only two of these appear to be actively pursued at present, as outlined in Fig. 1. In this figure the solid lines represent measurable energy levels of the chiral molecule under consideration, whereas the dotted lines refer to the potential energy

[a] *Physical Chemistry, ETH Zurich, CH-8093 Zurich, Switzerland. E-mail: martin@quack.ch; Fax: +41-44-632-1021; Tel: +41-44-632-4421*
[b] *Swiss Light Source, PSI Villigen, CH-5232 Villigen, Switzerland*

† Electronic supplementary information (ESI) available. See DOI: 10.1039/c6cp01493c

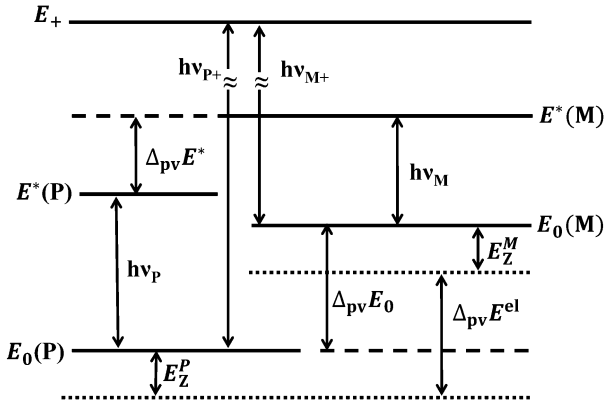

Fig. 1 Scheme of energy levels including parity violation in 1,2-dithiine (not to scale), see also ref. 44 and 47.

minima including the parity violating potential.[44] In theory the measurable energy represented by the solid lines would be obtained from the expectation values of the multidimensional parity violating potential in the quantum state considered, added to the energy eigenvalues of that state as computed from parity conserving ordinary molecular quantum mechanics[9,41,42] (see also Section 2).

In a first experimental scheme originally proposed by Letokhov and coworkers[30,49] one measures the difference in line positions, say, in the infrared spectrum of the separate enantiomers ($h\nu_M - h\nu_P$ in Fig. 1). This provides the difference ($\Delta_{pv}E^* - \Delta_{pv}E_0$) between two parity violating energy differences ($\Delta_{pv}E^*$ and $\Delta_{pv}E_0$) in two different energy levels. Early attempts towards such experiments were reported by Kompanets *et al.*[49] and Arimondo, Glorieux and Oka[50] (both unsuccessful). The work of Kompanets *et al.* on CHFClBr was further pursued by our group using high resolution microwave and infrared spectroscopy in molecular beams with detailed rovibrational analyses in order to identify suitable lines for detecting parity violation in these spectra.[57] These results of our group were subsequently used to carry out experiments at very high resolution by the Paris group[58] achieving about $\Delta\nu/\nu \approx 10^{-13}$ relative uncertainty, compared to theoretical predictions of shifts of the order $\Delta\nu/\nu \simeq 10^{-16}$, ref. 39–42. Recent progress by two groups following this scheme currently can be seen from ref. 59 and 60. One can estimate that successful experiments of this kind might be possible in the near future for chiral molecules involving very heavy atoms which have relatively large values of $\Delta_{pv}E$ because of the well-known scaling with atomic number.[35–48,61] Here it must be noted that atomic spectroscopy has already been successful to detect parity violation for very heavy atoms such as Cs, Bi *etc.*,[62–67] where a current limitation in the fundamental analysis actually results from uncertainties in the theory for such heavy-atom systems, which will be also a drawback if such experiments are successful on related molecules (see ref. 9 and 29 for a discussion). Another drawback of this first scheme is that it cannot provide $\Delta_{pv}E_0$ (or $\Delta_{pv}E^*$) separately. Also, this scheme requires the synthesis of separate enantiomers. We shall not discuss this scheme further here.

In the second scheme, proposed in ref. 52, one uses an excited intermediate level of well-defined parity (marked E_+ for positive parity in Fig. 1) which can be reached by electric dipole transitions from both enantiomers (marked $h\nu_{P+}$ and $h\nu_{M+}$ in Fig. 1). Then one can obtain $\Delta_{pv}E_0$ by a combination difference ($h\nu_{P+} - h\nu_{M+}$). Alternatively, one can use a time dependent variant of this scheme whereby a sequence of two electric dipole transitions to a superposition state of the two enantiomers is prepared. This superposition state has a well-defined parity initially (say, with a probability $p_-(t = 0) = 1$), which evolves in time according to eqn (2) for the complementary population of the state of positive parity detectable with high sensitivity on a "zero background"[9,52]

$$p_+(t) = 1 - p_-(t) = \sin^2(\pi\Delta_{pv}Et/h). \quad (2)$$

Here, we use the notation $\Delta_{pv}E$ for some general quantum state which may be the ground state (then one has $\Delta_{pv}E = \Delta_{pv}E_0$), the excited state with $\Delta_{pv}E = \Delta_{pv}E^*$ in Fig. 1, or some other selected quantum state. Recent detailed theoretical simulations have shown the feasibility of such experiments, in principle, for the realistic, simple chiral molecule ClOOCl.[68,69] Furthermore the experimental proof of principle has been demonstrated for the simple achiral molecule NH_3, where the current experimental sensitivity indicates that parity violating energy differences on the order of about 100 aeV or (hc) 10^{-12} cm^{-1} corresponding to about $\Delta_{pv}H_0^{\ominus} = 10^{-11}$ J mol^{-1} should be detectable with the existing set-up.[70] Such values are predicted for chiral molecules with atoms no heavier than sulfur or chlorine[71] which is a great advantage for a future theoretical analysis of experiments with very high accuracy[9,44] in addition to the advantage of providing separate values for individual $\Delta_{pv}E$. Another advantage of the second scheme is that experiments can be carried out on racemic mixtures as well as on separate enantiomers.

We should note that a general condition for both experimental schemes is that the parity violating energy difference $\Delta_{pv}E$ is much larger than the tunneling splitting $\Delta E_\pm$ calculated using the hypothetical symmetrical (parity conserving) Hamiltonian, thus

$$|\Delta_{pv}E| \gg |\Delta E_\pm|. \quad (3)$$

Indeed, this condition is a necessary requirement for an energy level scheme as in Fig. 1 to be applicable at all. The inequality (3) does not hold for chiral molecules such as HOOH and HSSH[9,48,72] but has been predicted theoretically to be fullfilled for ClOOCl[68,69] and ClSSCl,[71] for example, and also for the case of 1,2-dithiine to be studied here.

Current spectroscopic techniques result in some limitations on the complexity of the chiral molecules which can be studied. Also spectroscopically accessible states of well-defined parity must be identified by appropriate high resolution analyses. Such states can be found in electronically excited states, for instance, in molecules such as difluoroallene[76] or they can be found in the electronic ground state at energies near or above the barrier for stereomutation as shown for ClOOCl.[68,69] One can thus identify the following steps in preparing for experiments on $\Delta_{pv}E$ in chiral molecules.

(1) Identify suitable chiral molecules by approximate exploratory theoretical calculations, demonstrating sufficiently large absolute

values $|\Delta_{pv}E|$ to be measurable and small absolute values $|\Delta E_{\pm}|$ for the tunneling splitting such that the inequality (3) holds.

(2) Carry out the necessary synthesis and exploratory high resolution spectroscopic analyses.

(3) Identify spectroscopic lines suitable to carry out the experiment according to the second scheme.

(4) Carry out the experiment to measure $p_+(t)$ according to eqn (2) with significant accuracy to provide $\Delta_{pv}E$.

(5) Analyse highly accurate experimental results of $\Delta_{pv}E$ by means of highly accurate theoretical calculations to extract fundamental parameters of the standard model of particle physics (SMPP) such as the Weinberg parameter which may be significantly different in experiments of high energy physics and "low energy atomic and molecular physics" spectroscopic experiments, for instance.[9]

In the present work we show that the chiral molecule 1,2-dithiine is a possible candidate for experiments on $\Delta_{pv}E$ by carrying out in essence steps 1 and 2 of the program listed above. In Section 2 we show by theoretical calculations that 1,2-dithiine has a favourable, large absolute value $|\Delta_{pv}E|$ and a very small ground state tunneling splitting $|\Delta E_{\pm}|$ satisfying the inequality (3). Furthermore the barrier for stereomutation is calculated to be low enough for states above the barrier with well-defined parity to be accessible by the currently available high resolution lasers in the infrared range.[70]

1,2-Dithiine as shown in Fig. 2 is a six membered chiral ring compound of C_2 symmetry which has been synthesized in ref. 77 and 78 and since this early synthesis combined with the finding that 1,2-dithiines occur as natural products[79,80] there have been substantial experimental and theoretical studies, of which we can cite here only a selection[81–89] including also in particular a review[82] and a recent theoretical study of parity violation in the series of molecules starting with dioxine ($C_4H_4O_2$) leading to 1,2-dithiine and the higher members of this series with Se, Te, and Po[83] and studies of electronic structure and antiaromaticity.[84–89] Disulfides in general have been discussed as candidates for experimental studies of parity violation by us before,[71,72] recently extended to the slightly more complex trisulfane.[90] 1,2-Dithiine is spectroscopically already quite complex but recent experimental progress has made molecules of similar complexity such as pyridine, pyrimidine, fluorobenzene, chlorobenzene,[91] and phenol as well as naphthalene and azulene accessible to high resolution infrared spectroscopic analyses (see ref. 91, and references cited therein).

The outline of the present paper is briefly as follows. In Section 2 we present the theory for tunneling and parity violation. In Section 3 we discuss our experiments on the synthesis, high resolution THz (FTIR) and also GHz spectroscopy. In Section 4 we discuss the spectroscopic assignments and in Section 5 an extended rotational analysis of the ground state of 1,2-dithiine as well as of three of the stronger fundamentals ν_{22} (ν_0 = 623.3121 cm^{-1}), ν_{17} (ν_0 = 1308.8724 cm^{-1}) and ν_3 (ν_0 = 1544.9004 cm^{-1}) demonstrating the feasibility of such analyses for this chiral molecule, for which the infrared spectra have not been analysed at high resolution before, while some limited microwave data existed already[75] with a total of only 15 microwave lines for the normal isotopomer. We conclude with a detailed discussion and an outlook towards the feasibility of experiments to measure parity violation in this chiral molecule. A preliminary report on the present research has been given in ref. 92–94.

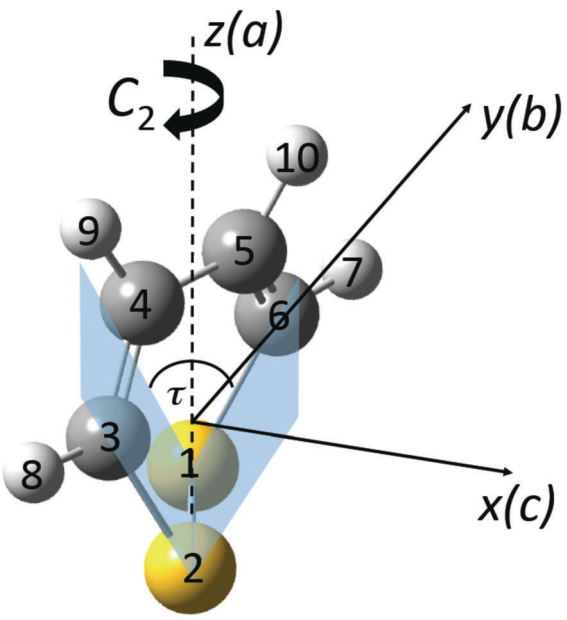

Fig. 2 Perspective drawing of the molecular structure of 1,2-dithiine ($C_4H_4S_2$) and principal axes together with the general atom numbering scheme (P enantiomer, sulfur yellow (1,2), carbon black (3,4,5,6) and hydrogen light grey (7,8,9,10)).

2 Theory

The interesting non-planar structure of 1,2-dithiine is shown in Fig. 2. The equilibrium structure of the electronic ground state ($\tilde{X}$ ^{1}A) was optimized at the MP2/cc-pVTZ, MP2/cc-pVQZ and CCSD(T)/cc-pVTZ levels of theory. These computations were carried out using the Gaussian 09[73] and Molpro[95,96] program packages. The planar ring structure would formally have 8 π-electrons and thus would be antiaromatic and destabilized. However, this effect is reduced by avoiding the planar geometry. The predicted ring structure possesses C_2 symmetry and the optimized structural parameters are summarized in Table 1 for the equilibrium geometry. The calculated structure agrees well with an experimental r_s-structure from microwave spectroscopy.[75] The corresponding theoretical rotational constants are compared with the experimental results in Section 4 below in more detail. Again, the overall agreement is remarkably good. The only structural parameter which shows a large difference between experiment and theory is the S–S bond length differing by about 3 pm when compared with the CCSD(T) results, where one must consider also the different physical meanings of r_s and r_e structures. The calculated harmonic wavenumbers $\tilde{\omega}_i$, the vibrational fundamentals $\tilde{\nu}_i$ (with anharmonic corrections) and the predicted integrated band strengths (in km mol^{-1}) are given in Table 2. The most intense fundamental $\tilde{\nu}_{22}$ = 623 cm^{-1} corresponds to a CH

Table 1 Optimized equilibrium structure parameters (r_e in pm, angles in degrees) of the ground electronic state $\tilde{X}\ ^1A_1$ of 1,2-dithiine (C_2 symmetry, atom numbering as in Fig. 2). The MP2 calculations were done using the Gaussian 09 package[73] and the CCSD(T) calculations using the Molpro program package.[74] (We indicate: method/basis set as shown)

	MP2/ cc-pVTZ	MP2/ cc-pVQZ	MP2/ cc-pV5Z	CCSD(T)/ cc-pVTZ	Exp.[a]
$r(S_1C_6)$	176.21	175.58	175.17	177.59	175.9(4)
$r(S_1S_2)$	206.23	204.77	203.88	208.35	205.1(3)
$r(C_5C_6)$	135.08	134.91	134.93	134.89	135.3(3)
$r(C_4C_5)$	144.71	144.44	144.36	146.12	145.1(1)
$r(C_6H_7)$	108.21	108.16	108.16	108.32	
$r(C_5H_{10})$	108.25	108.19	108.17	108.41	
$\alpha(C_6S_1S_2)$	97.99	98.12	98.19	98.27	98.7(2)
$\alpha(S_1C_6C_5)$	121.39	121.17	121.07	121.88	121.4(2)
$\alpha(C_4C_5C_6)$	124.18	124.14	124.07	124.40	124.2(2)
$\alpha(S_1C_6H_7)$	116.65	116.77	116.90	116.09	
$\alpha(C_6C_5H_{10})$	117.85	117.87	117.90	118.14	
$\tau(C_6S_1S_2C_3)$	54.99	55.31	55.59	53.25	53.9
$\tau(S_2S_1C_6H_7)$	141.14	141.07	141.02	141.82	
$\tau(S_2S_1C_6C_5)$	−42.27	−42.37	−42.51	−41.11	−41.2
$\tau(S_1C_6C_5H_{10})$	−177.25	−177.18	−177.08	−177.85	

[a] Experimental structural parameters from ref. 75 (r_s structure).

"out-of-plane" bending mode, followed by the ring twisting fundamental $\tilde{\nu}_{24}$ = 214 cm^{-1} and the CH "in-plane" bending fundamental $\tilde{\nu}_{17}$ = 1303 cm^{-1} where "out-of-plane" and "in-plane" have obviously only approximate meaning for this non-planar molecule. Further intense absorptions arise from the CC stretching polyads and the CH stretching polyads.

The twisted structure with a dihedral angle $\tau(C_6–S_1–S_2–C_3)$ of 53.25 degrees gives rise to P and M enantiomorphism, with a

Table 2 Calculated harmonic wavenumbers $\tilde{\omega}_i$ (in cm^{-1}), IR intensities (in km mol^{-1}), and anharmonic fundamentals $\tilde{\nu}_i$ (in cm^{-1}) of 1,2-dithiine as calculated using the Gaussian 09 package[73]

Mode	Symmetry	$\tilde{\omega}_i$ (MP2/ cc-pVTZ)	Intensity	$\tilde{\nu}_i$ (MP2/ cc-pVTZ)	Approximate description
1	A	3226	8.495	3085	CH stretches
2	A	3204	0.206	3077	CH stretches
3	A	1568	11.063	1522	CC stretches
4	A	1390	4.468	1349	CH in-plane bends
5	A	1181	0.098	1164	CH in-plane bends
6	A	997	2.670	981	C_2C_3 stretch
7	A	938	0.814	920	CH out-of-plane bends
8	A	780	3.451	767	CH out-of-plane bends
9	A	740	4.977	728	CS sym. Stretches
10	A	573	0.100	565	SS stretch, CH out-of-plane bends
11	A	523	0.068	516	SS stretch, CH out-of-plane bends
12	A	448	0.243	441	CCC in-plane bends
13	A	204	0.001	200	Ring pucker
14	B	3221	5.420	3115	CH stretches
15	B	3197	0.882	3075	CH stretches
16	B	1610	0.210	1563	CC stretches
17	B	1329	14.809	1303	CH in-plane bends
18	B	1184	1.162	1166	CH in-plane bends
19	B	929	0.139	910	CH out-of-plane bends
20	B	858	2.711	847	CCC in-plane bends
21	B	702	1.495	684	CS asym. stretches
22	B	632	92.517	623	CH out-of-plane bends
23	B	315	0.083	312	CSS in-plane bends
24	B	214	12.041	214	CCC out-of-plane bends

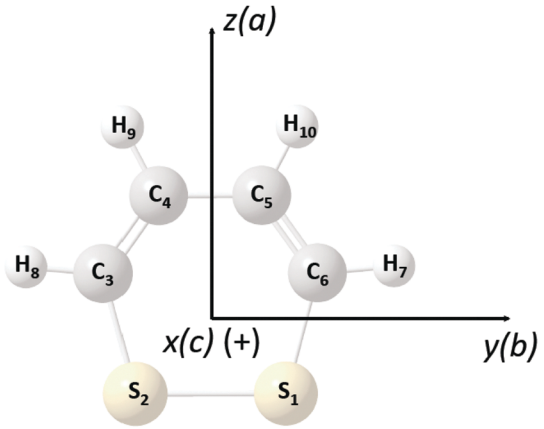

Fig. 3 Transition state and alternative atom numbering in 1,2-dithiine.

planar structure of C_{2v} symmetry being the transition state for interconversion between the two enantiomers (Fig. 3 and Table 3). Formally, this corresponds to the *cis*-transition state of general disulfides with internal rotation.[71,72] The S–S bond length is elongated to 217.8 pm (CCSD(T)/cc-pVDZ level) and one finds as angles $\alpha(C_6–S_1–S_2)$ = 104.43° and $\alpha(S_1–C_6–C_5)$ = 129.72° for the transition state which are the only structural parameters apart from the obvious dihedral angles differing substantially from the equilibrium structures. The transition state as calculated at the CCSD(T)/cc-pVQZ level of theory is found to be about 2500 cm^{-1} above the potential minimum (without vibrational zero-point energy correction). The planar structure is shown in Fig. 3 which also indicates the atom numbering with C_6, S_1, S_2, C_3, C_4, C_5 and H_7, H_8, H_9, H_{10}. The structural parameters are summarized in Table 3 and the harmonic wavenumbers of the transition state are given in Table 4 with the species in C_{2v} symmetry.

The parity-conserving electronic (V_{el}) and parity-violating potentials (E_{pv}) computed along the IRC interconversion path are given in Fig. 4. E_{pv} was computed with our recently developed[44,97] coupled-cluster singles and doubles linear response approach (CCSD-LR) using the Zurich version of the PSI3 program.[98] E_{pv} is obtained as a linear response function of

Table 3 Optimized molecular structure parameters (r_e in pm, angles in degrees) of the planar transition state for the stereomutation of 1,2-dithiine (C_{2v} symmetry). The MP2 calculations were done using the Gaussian 09 package[73] and the CCSD(T) calculations using the Molpro program package[74]

	MP2/cc-pVTZ	MP2/cc-pVQZ	CCSD(T)/cc-pVDZ
$r(S_1C_6)$	175.36	174.81	177.97
$r(S_1S_2)$	212.78	211.46	217.82
$r(C_5C_6)$	134.18	133.95	135.75
$r(C_4C_5)$	145.37	145.18	147.54
$r(C_6H_7)$	108.30	108.24	109.94
$r(C_5H_{10})$	108.10	108.04	109.75
$\alpha(C_6S_1S_2)$	104.73	104.88	104.43
$\alpha(S_1C_6C_5)$	129.57	129.49	129.72
$\alpha(C_4C_5C_6)$	125.70	125.63	125.85
$\alpha(S_1C_6H_7)$	109.87	109.85	109.75
$\alpha(C_6C_5H_{10})$	116.67	116.71	117.01

Table 4 Calculated harmonic wavenumbers $\tilde{\omega}_i$ (in cm^{-1}) of the planar transition state for the stereomutation of 1,2-dithiine ($i = \sqrt{-1}$) as calculated using the Gaussian 09 program package[73]

Mode	Symmetry	$\tilde{\omega}_i$ (MP2/cc-VTZ)	$\tilde{\omega}_i$ (MP2/cc-pVQZ)
1	A_1	3233	3231
2	A_1	3202	3202
3	A_1	1628	1626
3	A_1	1403	1402
5	A_1	1209	1208
6	A_1	985	985
7	A_1	729	732
8	A_1	513	515
9	A_1	458	462
10	A_2	927	928
11	A_2	746	743
12	A_2	503	509
13	A_2	i162	*i*168
14	B_1	926	926
15	B_1	642	640
16	B_1	263	264
17	B_2	3222	3221
18	B_2	3198	3199
19	B_2	1645	1644
20	B_2	1341	1342
21	B_2	1213	1212
22	B_2	850	851
23	B_2	678	681
24	B_2	314	315

the coupled cluster wavefunction with an effective one-electron spin–orbit coupling serving as a static perturbation. We employed a decontracted cc-pVDZ basis set augmented with a set of steep s and p functions. Details of the theoretical approach have been described in ref. 44.

Based on our calculations, and as can be seen from Fig. 4, we predict the P-enantiomer to be stabilized with respect to the M-enantiomer. The computed value of E_{pv} for P-1,2-dithiine is $E_{pv}/(hc) = -5.72 \times 10^{-12}$ cm^{-1}. The signed electronic parity violating the energy difference $\Delta_{pv}E^{el}$ between the two enantiomers as defined by eqn (4) is obtained to be

$$\Delta_{pv}E^{el}(q_e) = E^{el}_{pv}(q_M) - E^{el}_{pv}(q_P) = (hc)\ 11.44 \times 10^{-12}\ cm^{-1} \qquad (4)$$

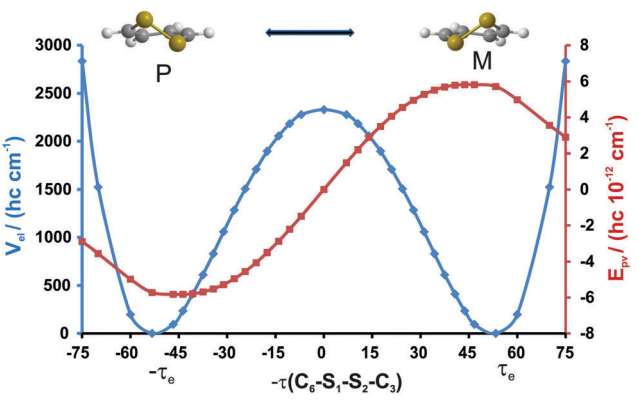

Fig. 4 Parity-violating potential E_{pv} (CCSD-LR/cc-pVDZ) and the parity-conserving potential V_{el} (CCSD(T)/cc-pVTZ) computed along the IRC interconversion path for 1,2-dithiine. The P enantiomer has negative values of $-\tau$, the M enantiomer has positive values of $-\tau$ (in degrees °).

where q stands for the reaction coordinate along the IRC path. The value for $\Delta_{pv}E^{el}(q_e)$ is remarkably large and is related to the parity violating potential having its maximum as a function of the dihedral angle near the equilibrium geometry. It can be compared with the very similar values in the range $(11 \pm 1) \times 10^{-12}$ cm^{-1} obtained with several methods in ref. 83.

In order to estimate the ground-state tunneling splitting ($\Delta E_{\pm}$) the $\tau(C_6–S_1–S_2–C_3)$ dihedral angle (denoted by τ) was selected to be the reaction coordinate describing the interconversion of the two puckered enantiomers through a planar transition state. For every energy value as a function of τ the remaining internal coordinates were optimized at the MP2/cc-pVTZ level of theory and the resulting structures were then used for single-point CCSD(T)/cc-pVQZ electronic structure computations. This definition of the reaction coordinate was justified by MP2/cc-pVTZ IRC computations, where the resulting IRC path connecting the planar transition state with the two enantiomeric potential minima was found to be almost identical to the 1D MP2/cc-pVTZ reaction path following simply a variation of τ. The structural parameters as a function of the reaction coordinate values q_i and the harmonic wavenumbers as a function of q are given in the ESI.†

We employed the quasi-adiabatic channel reaction path Hamiltonian approach (RPH)[99–101] to compute the tunneling splittings $\Delta E_{\pm}$. In conjunction with the Born–Oppenheimer potential (CCSD(T)/cc-pVQZ, see the dashed line in Fig. 5) we used Cartesian coordinates, energy gradients and harmonic force fields (all of these quantities were obtained at the MP2/cc-pVTZ level of theory) along the reaction path to generate the lowest quasi-adiabatic channel potential (Fig. 5, solid line). The barrier heights are 2529 cm^{-1} (Born–Oppenheimer potential) and 2559 cm^{-1} (lowest quasi-adiabatic channel potential). The RPH energy levels corresponding to the lowest quasi-adiabatic channel potential are given in Table 5. It can be seen from Table 5 that the tunneling splittings increase as the energy

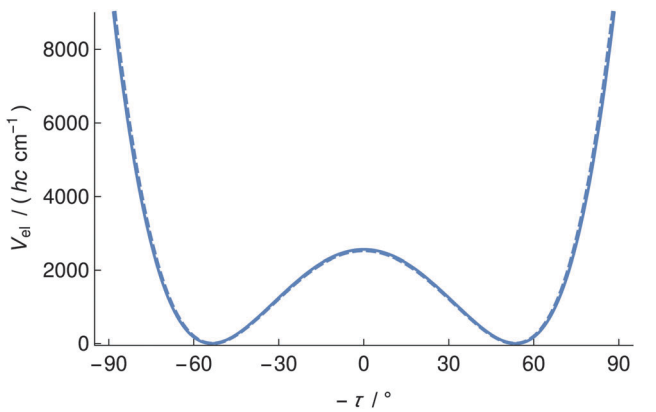

Fig. 5 Potential energy function corresponding to the 1D reaction path (see the text for discussion). The electronic Born–Oppenheimer (dashed line) and the lowest quasi-adiabatic channel potentials (solid line) are referred to their respective minima being separated by the 23D zero point energy (*hc*) 14 882 cm^{-1} and τ_{CSSC} denotes the $C_6–S_1–S_2–C_3$ dihedral angle. Using the shift by this large difference in reference energies, the two effective potentials almost coincide.

Table 5 RPH energy levels for the lowest adiabatic channel of 1,2-dithiine as $E/(hc)$ in cm^{-1}. The energy levels with even parity are given, the splittings as separation from the odd parity levels are given in parentheses. All levels are given with reference to the zero-point level (101.53 cm^{-1} above the minimum of the channel)

v = 0	0.00 (4×10^{-25})	v = 10	1860.60 (1.4×10^{-4})
v = 1	202.39 (3×10^{-22})	v = 11	2019.19 (4.2×10^{-3})
v = 2	401.84 (7×10^{-20})	v = 12	2169.37 (0.10)
v = 3	598.16 (7×10^{-18})	v = 13	2307.68 (1.80)
v = 4	791.14 (4×10^{-17})	v = 14	2421.75 (17.48)
v = 5	980.51 (8×10^{-15})	v = 15	2514.78 (52.76)
v = 6	1166.00 (2×10^{-12})	v = 16	2636.09 (69.83)
v = 7	1347.23 (1.4×10^{-9})	v = 17	2779.88 (76.93)
v = 8	1523.79 (8.4×10^{-8})	v = 18	2936.34 (82.13)
v = 9	1695.15 (3.8×10^{-6})	v = 19	3102.76 (86.59)

levels approach the barrier. At v = 12, about 2170 cm^{-1} above the minimum of the channel and still almost 400 cm^{-1} below the barrier the tunneling splitting of 0.1 cm^{-1} would be easily measurable in the infrared region. This large value is quite remarkable in view of the essentially pure "heavy atom" motion for the tunneling process.

Since the tunneling splittings of the lowest tunneling doublets are very small owing to the high interconversion barrier and large effective tunneling mass, their direct variational computation is not easily possible due to numerical limitations. In order to estimate $\Delta E_{\pm}$ we invoked an extrapolation technique that has been successfully used for the calculation of small tunneling splittings in ClSSCl.[71] This method resulted in a ground-state tunneling splitting of $\Delta E_{\pm}/(hc) = 4 \times 10^{-25}$ cm^{-1}. We have also calculated the expectation value of $\Delta_{pv}E$ in the torsional ground state and found it to differ by less than 10% from $\Delta_{pv}E^{el}$. Thus the parity violating energy difference $\Delta_{pv}E$ clearly exceeds the tunneling splittings for the hypothetical symmetrical potential by many orders of magnitude and 1,2-dithiine is a suitable candidate for measuring $\Delta_{pv}E$ by the technique proposed in ref. 52 from this point of view. We shall discuss further spectroscopic aspects in the following sections.

3 Experimental

3.1 Synthesis of 1,2-dithiine

1,2-Dithiine was synthesized according to the scheme in Fig. 6 using a procedure which is a modification of ref. 81, as described here, because the original procedure from ref. 81, which was tried as well, did not give quite satisfactory results in step c.

1,4-Bis(trimethylsilyl)buta-1,3-diyne (2). 1,4-Bis(trimethylsilyl)-buta-1,3-diyne (**2**) was obtained according to the method of ref. 102. The yield was 75% and the purity was 97% as controlled by GC-MS.

1,4-Bis(benzylthio)buta-1*Z*,3*Z*-diene (3). 1,4-Bis(benzylthio)buta-1*Z*,3*Z*-diene (**3**) could be obtained following ref. 81. No recrystallisation was carried out. The reaction product was used without further purification. The yield was 80% and the purity was 90% as obtained by NMR. The NMR-shifts correspond to the values given in ref. 81.

1,4-Bis(acetylthio)buta-1*Z*,3*Z*-diene (4). 1,4-Bis(acetylthio)buta-1*Z*,3*Z*-diene (**4**) could be obtained by placing 6.5 g (22 mmol) of compound **3** (Fig. 6) in a 3-neck round bottom flask equipped

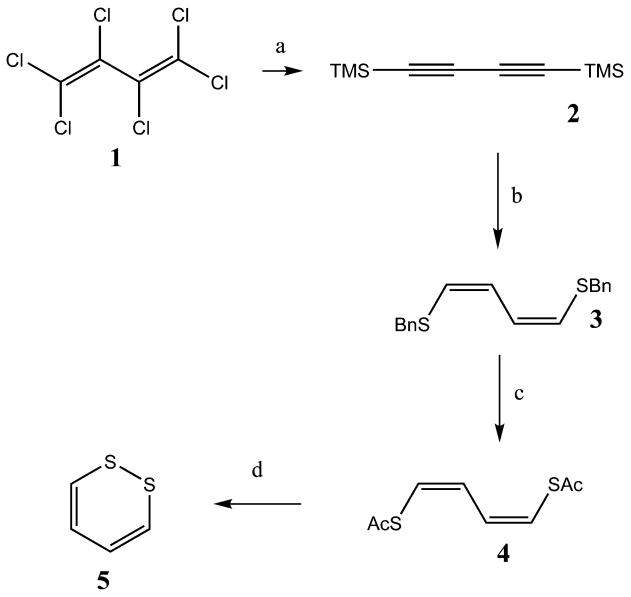

a) 4 equivalent of n-buthyllithium at -78 °C, then adding 2 equivalents of trimethylchlorosilane at 0 °C. The reaction was carried out in tetrahydrofurane,
b) Sodium and benzylmercaptane at 0°C in methanol, then reflux for 48 h,
c) In liquid ammonia with sodium and ammoniumchloride at -78 °C,
d) Potassium hydroxide in methanol at 0 °C and iodine in Methanol at -78 °C.

Fig. 6 Scheme for the synthesis of 1,2-dithiine.

with a mechanical stirrer, a dry ice cooler, a funnel for solids and a 3-way valve (connection to a balloon, the apparatus and a tube to the fume hood) and slowly condensate 300 ml of ammonia at −78 °C into the reaction flask. After adding 4.1 g (186 mmol) of freshly cut sodium the colour turned to dark blue and the reaction mixture was stirred at −78 °C overnight. Adding 20 g of ammonium chloride under a mild stream of nitrogen dried over phosphorous pentoxide the blue colour began to disappear. To remove ammonia from the liquid remaining in the flask, the cooling bath was replaced by a water bath and the gas was allowed to evaporate. After hydrolysing with 200 ml of deionised water the reaction mixture was extracted 4 times with 100 ml of diethyl ether where no hydrolysis product could be detected by GC-MS. The water phase was transferred into a 500 ml round bottom flask, then we added 40 ml (424 mmol) of acetic anhydride. After cold filtration the product was washed twice with cold water to give a pale yellow solid which was dried overnight at 50 °C and 50 mbar. The yield was 78% and the purity was determined by GC-MS[77] to be 90%.

1,2-Dithiine (5). 1,2-Dithiine (**5**) could be obtained according to the procedure of ref. 82. Only the workup differs from the method described therein. After extraction the solvent was removed at −78 °C and 10^{-3} mbar. The red oil was then condensed in a trap cooled with liquid nitrogen to give the expected 1,2-dithiine. This product was used without further purification. The substance is light sensitive. The yield was 55%

and the purity as determined by GC-MS was about 95%. Due to photochemical and further reactions impurities develop over time in the samples used for the spectroscopy. In particular, thiophene was observed by infrared spectroscopy. However, in the high resolution spectra the identity of the lines assigned to 1,2-dithiine was obvious from the spectra, also confirming the identity of the main substance.

3.2 GHz measurements of 1,2-dithiine

The ground state pure rotational spectra of 1,2-dithiine have been recorded between 65 and 117 GHz using our GHz spectrometer described in detail in ref. 103 and only slightly modified here. It consists of an Agilent synthesizer (E8257D PSG, Agilent Technologies Option 520 UNX) working in the range 250 kHz to 20 GHz with a frequency resolution of 0.001 Hz and frequency locked to a 10 MHz-rubidium standard (FS725, Stanford Research Systems) for short-term stability and to a GPS standard (TM-4, Spectrum Instruments Inc.) for long-term stability. The signal is frequency multiplied by a factor of 6 (S10MS-AG, OML Inc.) and coupled out to free space *via* a conical W-band antenna (QWH-WCRR, QuinStar Technology Inc.) leading to an operation in the frequency range of 67 to 118 GHz. The beam is focused through Teflon lenses into a 2.5 m path length glass cell equipped with two Teflon windows and mounted in a Brewster angle to the incoming and outcoming beam. Finally the beam is detected with a two-channel indium antimonide (InSb) bolometer [QFI/2(2),QMC Instruments Ltd.] after passing through a second Teflon lens. All transitions were measured using the frequency modulation technique (second harmonic lock-in detection) with a modulation frequency of 50 kHz.

The gas sample was prepared by introducing the vapour at a pressure of approximately 0.025 mbar (measured using two Baratron gauges 627B.1T and 627B11M, MKS Instruments) from a liquid sample to the 2.5 m glass cell, which was covered by an aluminum foil to prevent 1,2-dithiine from photochemical decomposition due to exposure to daylight. A typical measured linewidth (full-width-at-half-maximum) at 100 GHz was close to 200 kHz. Fig. 7 shows a survey spectrum in the GHz range.

3.3 FTIR measurements of 1,2-dithiine

The FTIR spectrum of 1,2-dithiine has been recorded using our Fourier transform spectrometer Bruker IFS 125 HR Zürich prototype (ZP 2001) in the region 600–3200 cm^{-1}. The Zurich FTIR setup is described in detail in ref. 106–109. The effective resolution ranged from 0.001 cm^{-1} in the range 600–1000 cm^{-1}, close to the Doppler width (FWHM), which ranged from 0.0006 cm^{-1} at 500 cm^{-1} to 0.0036 cm^{-1} at 3000 cm^{-1}. A White-type cell with path lengths ranging from 3.2 m up to 19.2 m and a 3 m glass cell were used for room temperature (295 K) measurements. The sample pressure measured using a MKS Baratron was varied between 0.1 and 1 mbar. All spectra were self-apodized. Table 6 shows the measurement parameters. Apertures from 0.8 mm to 1.0 mm were used. The spectra were calibrated with OCS (600–1300 cm^{-1})[104,109] and water (1280–1365 cm^{-1}).[105] In general, the calibrated wavenumbers are estimated to be accurate within 0.0002 cm^{-1}. The resolutions specified in Table 6 correspond to nominal bandwidths defined as $0.9 \times 1/d_{MOPD}$.[109] The data given in the ESI† correspond to calibrated wavenumbers. Due to the instability of 1,2-dithiine some impurities arising from reaction products such as thiophene have been identified in the spectra. As a survey we also measured further spectra covering the range 800–5000 cm^{-1} at low resolution.

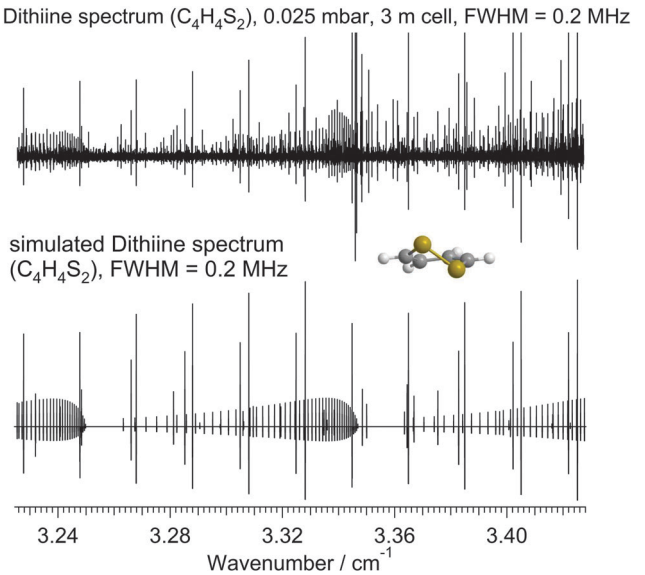

Fig. 7 Rotational survey spectrum of the ground state of 1,2-dithiine in the range 3.23–3.42 cm^{-1} (97–102.5 GHz). The spectrum is frequency modulated. One recognizes the 600 MHz spacing of the strongest adjacent K_a lines. The pressure was p = 0.025 mbar, the path length was l = 2.5 m and the temperature was T = 295 K. The upper trace shows the measured rotational spectrum and the lower trace a simulation using the parameters in Table 9.

Table 6 Measurement parameters for the 600–3600 cm^{-1} region of the infrared spectrum of dithiine

Region/cm^{-1}	600–1000	1150–2200	2500–3600
Resolution/cm^{-1}	0.0008	0.001	0.001
Windows	KBr	KBr	KBr
Source	Globar	Globar	Tungsten
Detector	MCT	MCT	InSb
Beam splitter	Ge:KBr	Ge:KBr	Si:CaF_2
Opt. filter/cm^{-1}	550–1000	900–2500	550–5000
Aperture/mm	1.0	0.8	0.8
ν_{mirror}/(kHz)	40	40	40
Calib. gas	OCS[104]	H_2O[105]	OCS[104]

4 Rotational and rovibrational assignments

4.1 General aspects and symmetry considerations

Table 7 includes the character tables for the point group C_2, the molecular symmetry groups M_{S_2} and M_{S_4} including the possibility of tunneling following Longuet-Higgins[114] and the systematic notation of ref. 110 for the symmetry species indicating parity explicitly by + and −. We also show in Table 7 the notation for the C_{2v} symmetry group of the transition state and the induced

Table 7 Character table for the C_2 and M_{S_2} symmetry groups (upper table) and character table for the C_{2v} and $S_2^*(M_{S_4})$ symmetry groups (lower table). For the molecular symmetry group (M_{S_4}) (αβ) corresponds to the combined permutation of the symmetrically equivalent nuclei of the molecule and the upper right index of the symmetry species indicates parity (+ or −)[110–113]

C_2	M_{S_2}	E E	C_2 (αβ)	μ	J	K_aK_c	$n_{\Gamma v}$	$n_{\Gamma s}$	g	$\Gamma(M_{S_2})\uparrow M_{S_4}$
A	A	1	1	μ_z	J_z	ee, eo	13	10	10	$A^+ + A^-$
B	B	1	−1	μ_x, μ_y	J_x, J_y	oo, oe	11	6	6	$B^+ + B^-$

C_{2v}	$S_2^*(M_{S_4})$	E E	C_2 (αβ)	σ_{xz} (αβ)*	σ_{yz} E^*	μ	J	K_aK_c	$n_{\Gamma v}$	$n_{\Gamma s}$	g
A_1	A^+	1	1	1	1	μ_z		ee	9	10	10
A_2	A^-	1	1	−1	−1		J_z	eo	4	0	10
B_1	B^-	1	−1	1	−1	μ_x	J_y	oo	3	0	6
B_2	B^+	1	−1	−1	1	μ_y	J_x	oe	8	6	6

representations $\Gamma(M_{S_2})\uparrow(M_{S_4})$ which indicate the symmetries of the tunneling sublevels. The nuclear spin statistical weights g arising from the $2^4 = 16$ nuclear spin functions of the 4 protons (H_7, H_8, H_9, H_{10}) combined with the motional functions to Pauli allowed states are indicated for each symmetry. The combination of the rotational quantum numbers K_a and K_c for the asymmetric top in a totally symmetric vibronic level is given as well in Table 7, which also includes the number of vibrational modes of each symmetry ($n_{\Gamma v}$). According to the C_2 symmetry the modes with A symmetry generate *a*-type transitions and the modes with B symmetry generate *b*- and *c*-type transitions. In a more detailed description the modes with A symmetry can split into A_1 and A_2 symmetry and the modes with B symmetry into B_1 and B_2 symmetry in the planar transition state as shown in Tables 2 and 4. As a consequence the fundamentals with B symmetry generate mainly *c*-type transitions and weak *b*-type transitions if they correspond to out-of-plane modes in the planar transition state (B_1) or stronger *b*-type transitions than *c*-type transitions if they correspond to in-plane modes (B_2) in the planar transition state. We have also calculated the electric dipole transition moment components μ_a, μ_b and μ_c for the vibrational fundamentals in order to assist the assignments. The fundamentals with A symmetry generate weak *a*-type transitions if the modes correspond to out-of-plane modes (A_2) in the planar transition state because modes with A_2 symmetry are not infrared active. This is important with respect to the ring puckering mode ν_{13} which would correspond to an A_2 mode in the planar configuration. For that reason the fundamental ν_{13} is extremely weak. However, fundamentals with A symmetry generate strong *a*-type transitions if they correspond to in-plane modes in the planar transition state.

4.2 Assignment procedure

Fig. 7 shows part of the ground state rotational spectrum of 1,2-dithiine in the range 97–102.5 GHz. The assignment of the rotational transitions has been performed using the Pgopher program,[115,116] a Loomis–Wood assignment program, and the WANG program[117] up to $J = 50$. The infrared spectral region between 600 cm^{-1} and 1000 cm^{-1} as illustrated in Fig. 8 shows one strong absorption feature, and the region between 1150 cm^{-1} and 2200 cm^{-1} shows two strong absorption bands of 1,2-dithiine at

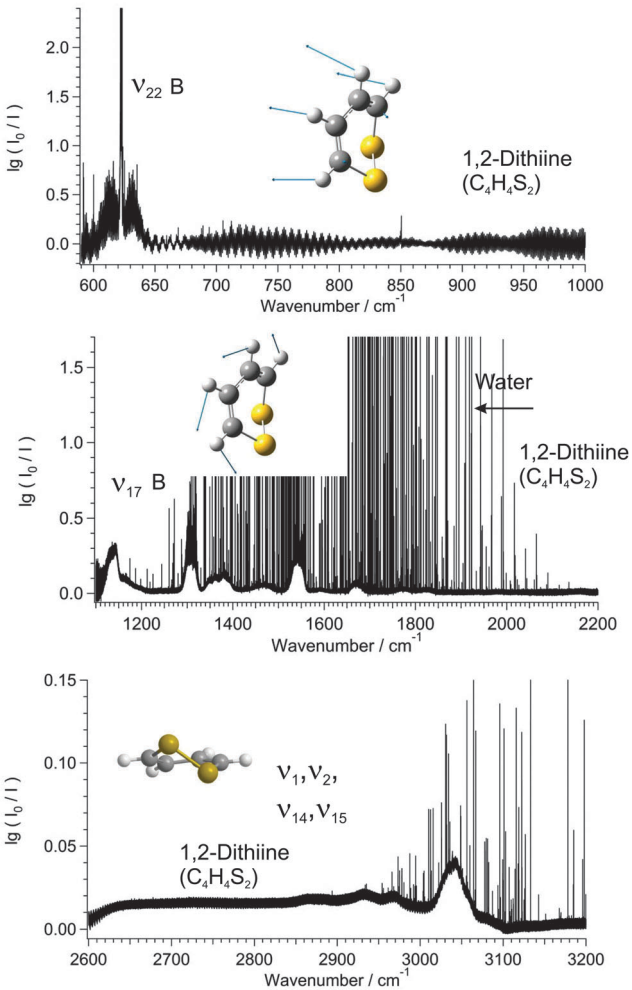

Fig. 8 Survey spectrum of 1,2-dithiine in the range 600–1000 cm^{-1} (upper panel), 1150–2200 cm^{-1} (middle panel) and 2600–3200 cm^{-1} (third panel). The 1150–2200 cm^{-1} range (middle panel) is dominated by strong water absorption lines. The decadic absorbance $lg(I_0/I)$ is shown as a function of wavenumber. The pressure was p = 0.7 mbar, the path length was l = 3 m and the temperature was T = 295 K. The standing wave pattern generates the broad base line waves in the 600–1000 cm^{-1} range. However, the width of these waves is 100 to 1000 times broader than the effective linewidth and therefore does not disturb the high resolution analysis.

1310 cm^{-1} and 1590 cm^{-1}. The strong sharp lines visible in Fig. 8 are due to water absorption lines. In the following description the term 'subband' or 'series' describes the transitions belonging to one K_a or K_c value. The assignment of the observed rovibrational transitions belonging to a particular subband consisting of P and R branches has been carried out efficiently using an interactive Loomis–Wood (LW) assignment program[118] (see also ref. 109 and 119) previously designed for linear molecules.[120–122] This limitation is, however, only superficial as the assignment program has been used successfully for several asymmetric top molecules: $CHClF_2$,[123,124] $CHCl_2F$,[108,125] CDBrClF,[106] pyridine, and pyrimidine.[126]

4.3 Ground state of 1,2-dithiine

1,2-Dithiine is an asymmetric rotor with C_2 symmetry, its only permanent electric dipole moment component lies along the

a-axis (μ_a = 1.85 D[75]), allowing transitions obeying *a*-type selection rules (eo ↔ ee and oe ↔ oo) for rotational transitions. The assignment of the rotational transitions observed here was assisted by using previously reported spectroscopic parameters from Gillies *et al.*,[75] which included only 15 transitions up to J = 5, K_a = 5. A total of 560 transitions were newly assigned up to $J \leq 50$ and $K_a \leq 19$ in the range of 65 to 117 GHz in the present work. The overview spectrum in Fig. 7 illustrates the rotational structure of 1,2-dithiine in the ground state such as the stronger ^{a}R-type transitions progressing nicely with separations between adjacent K_a lines by about 600 MHz, while the ^{a}Q-type transitions are overshadowed and clustered.

4.4 The ν_{22} band of 1,2-dithiine

The ν_{22} band of 1,2-dithiine at 623 cm^{-1} (Fig. 8) is the strongest band in the IR absorption spectrum of 1,2-dithiine and consists of *c*- and *b*-type transitions. A comparison with the FTIR spectra of the already analysed aromatic molecules naphthalene,[127] azulene[128] and phenol[129] illustrates that the ν_{22} fundamental of 1,2-dithiine corresponds to the strongest out-of-plane fundamentals of these aromatic molecules which are also dominated by strong Q branches due to *c*-type transitions. However, the planar aromatic molecules show no *b*-type transitions according to the C_{2v} symmetry. The *c*- and *b*-type transitions are not split until $K_c < 11$. The *c*-type series were identified as P, R and Q branches with ee ↔ oe and eo ↔ oo transitions. In addition, some *b*-type lines (around 20) above $K_c \geq 11$ have been assigned with ee ↔ oo and eo ↔ oe transitions. The spacing between two transitions of a *c*-type series is approximately 2A. The assignments were checked by comparison with ground state combination differences. Loomis–Wood diagrams of this band are shown in Fig. 9. The patterns of P and R branches of the *c*-type series are clearly visible in Fig. 9. The upper diagram shows the P branch and the middle diagram the R branch. The visible series are transitions where *c*- and *b*-types fall together. The lines have been assigned up to $J \leq 78$ and $K_a \leq 73$ and $K_c \leq 34$.

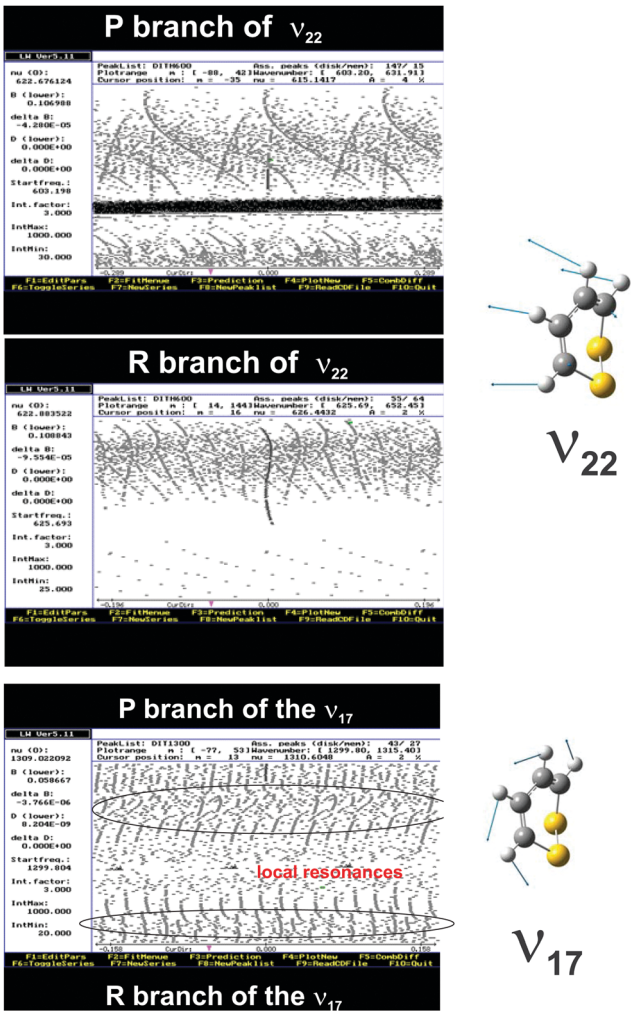

Fig. 9 Loomis–Wood (LW) diagrams of the *c*-type transitions of the ν_{22} band. The upper part shows the P branch and the middle part the R branch. The different K_c series are clearly visible which are unsplit *b*- and *c*-type transitions. The lower part shows the Loomis–Wood diagram of the *b*-type transitions of the ν_{17} band of 1,2-dithiine. The different K_a series of the P and R branches as well as the local resonances (crossings) are clearly visible.

4.5 The ν_{17} band of 1,2-dithiine

The observed spectrum of the ν_{17} fundamental of 1,2-dithiine at 1308 cm^{-1} clearly shows a characteristic *b*-type contour within the P and R branches and a *c*-type contour within the sharp center Q branch as shown in Fig. 8 (middle panel) and in more detail in Fig. 13. The shape of the *b*-type series is very similar to the shape of the *b*-type series assigned in the ν_{15} fundamental of fluorobenzene.[130] However, due to the C_{2v} symmetry of fluorobenzene the ν_{15} fundamental shows no *c*-type transition and therefore no visible Q branch. The ν_{17} band was chosen to be analyzed first, as a series of regularly spaced spectral patterns can be identified even through preliminary visual inspection. A simulated spectrum was generated using the estimated band center from inspecting the recorded high resolution data and the ground state spectroscopic parameters obtained from the analysis of the rotational spectra measured in the present work. The first attempt to assign the observed spectrum was based on the comparison with this simulated spectrum. The preliminarily assignments of the transitions were then confirmed by comparing the ground state combination differences with the GHz data. The simulated spectrum was refined by newly added assigned transitions and this process was continued in an iterative fashion until a few progressions of transitions were assigned. However, as the Loomis–Wood diagram of the P branch in Fig. 9 (lower part) illustrates, the *b*-type subbands are perturbed from J = 32 and onwards and therefore have only been assigned up to $J \leq 32$. A closer look at the Loomis–Wood diagram indicates that the ν_{17} state is perturbed from at least two states: one with higher energy and smaller rotational C constant and the second with lower energy and larger rotational C constant. Only *b*-type transitions were assigned. The *c*-type transitions are not rotationally resolved in this band.

4.6 The ν_3 band of 1,2-dithiine

The ν_3 band centered at 1544.9 cm^{-1} exhibits a strong absorption feature in the recorded spectrum as shown in the FTIR survey spectrum in Fig. 8 (middle trace). The strong sharp lines are due to water absorption. The assignment as the ν_3 fundamental is consistent with the predicted intensity of this band being the highest in the region of 1400–1600 cm^{-1} (Table 2). A few strong *a*-type transitions with low K_c values were readily assigned with the aid of Loomis–Wood diagrams and simulated spectra using ground state constants and the estimated band center allowed a better prediction of more transitions to be assigned. As for the ν_{17} band, local perturbations were encountered and the assignment of lines was carried out up to $J = 40$ only. Also, the relatively noisy background prevented the transitions with K_a larger than 10 from being assigned.

5 Results of the spectroscopic parameters and discussion

The rovibrational analysis has been carried out using Watson's *A* reduced effective Hamiltonians in the I^r representation (with the definitions of axes according to Fig. 2) up to sextic centrifugal distortion constants:[117,131]

$$\begin{aligned}\hat{H}^{v,v}_{rot} &= A_v\hat{J}_z^2 + B_v\hat{J}_x^2 + C_v\hat{J}_y^2 \\ &\quad - \Delta_J^v\hat{J}^4 - \Delta_{JK}^v\hat{J}^2\hat{J}_z^2 - \Delta_K^v\hat{J}_z^4 \\ &\quad - \frac{1}{2}\left[\left(\delta_J^v\hat{J}^2 + \delta_K^v\hat{J}_z^2\right), \left(\hat{J}_+^2 + \hat{J}_-^2\right)\right]_+ \\ &\quad + \Phi_J^v\left(\hat{J}^2\right)^3 + \Phi_{JK}^v\left(\hat{J}^2\right)^2\hat{J}_z^2 + \Phi_{KJ}^v\hat{J}^2\hat{J}_z^4 + \Phi_K^v\hat{J}_z^6 \\ &\quad + \frac{1}{2}\left[\left(\phi_J^v\left(\hat{J}^2\right)^2 + \phi_{JK}^v\hat{J}^2\hat{J}_z^2 + \phi_K^v\hat{J}_z^4\right), \left(\hat{J}_+^2 + \hat{J}_-^2\right)\right]_+ \end{aligned} \quad (5)$$

The angular momentum operators are given by $\hat{J}^2 = \hat{J}_x^2 + \hat{J}_y^2 + \hat{J}_z^2$ and $\hat{J}_\pm = \hat{J}_x \pm i\hat{J}_y$. The I^r representation was chosen to reduce correlations during the fit. The spectroscopic data were analyzed using the WANG program described in detail in ref. 117 and the SPFIT program.[132] The spectroscopic constants were fitted for each band separately according to the *A*-reduction.

5.1 Rotational analysis and parameters of the ground state of 1,2-dithiine

560 rotational transitions in the GHz region were combined with the 15 lines reported in ref. 75 in a joint least squares analysis. Using only the three rotational constants and five centrifugal distortion constants included in the adjustment, the overall d_{rms} of the fit consisting of 575 rotational transitions is remarkably low (less than 7 kHz, or 0.0000002 cm^{-1}). Table 8 lists all the spectroscopic parameters of the ground state of 1,2-dithiine. The rotational constants *A*, *B* and *C* obtained here compare well with those determined in the earlier microwave work. However, the previous study did not have a sufficient number of transitions (just a total of 15 lines) to accurately determine centrifugal distortion constants. In our work we observed more than 500 transitions and also covered a large range of the rotational spectrum with quantum numbers extending to $J \leq 50$ and $K_a \leq 19$, which led to a significant improvement in these centrifugal distortion constants. It was possible to observe intensity alternation in the spectra due to the nuclear spin statistical weights. According to Table 7 the expected intensity alternation in the rotationally resolved spectra of 1,2-dithiine is ee : eo : oo : oe = 10 : 10 : 6 : 6. Fig. 10 shows as an example a comparison of the strong R branch lines (upper trace) with simulations using the spectroscopic constants from Table 8 and using nuclear spin statistical weights (middle trace) and simulations without these weights (lower trace). The lower panel displays an enlarged part of the upper panel. Even for congested lines the effects of nuclear spin statistical weights are visible, confirming the assignments. This complete set of ground state rotational parameters (Table 8) plays an important role in the subsequent analysis of the dense rovibrational spectra in the preliminary assignment stage, especially when the upper state is perturbed.

Table 8 Equilibrium rotational constants A_e, B_e, C_e and spectroscopic parameters in cm^{-1} of the ground state of 1,2-dithiine in the *A*-reduction. The uncertainties are listed in parentheses in terms of 1σ in units of the last digits

	Theory (MP2/cc-pVTZ), t.w.	Expt. t.w.[a]
A_e/cm^{-1}	0.111061	0.111544[a]
B_e/cm^{-1}	0.103524	0.103980[a]
C_e/cm^{-1}	0.058925	0.058852[a]
	Ground state[75]	t.w. ground state[b]
A_0/cm^{-1}	0.1109554 (6)	0.110955440 (2)
B_0/cm^{-1}	0.1034997 (6)	0.103499682 (2)
C_0/cm^{-1}	0.05857394 (2)	0.058573904 (1)
$\Delta_J/10^{-6}$ cm^{-1}	0.0007 (2)	0.010663 (3)
$\Delta_{JK}/10^{-6}$ cm^{-1}	0.0037 (7)	0.013592 (9)
$\Delta_K/10^{-6}$ cm^{-1}	−0.002 (1)	−0.005986 (5)
$\delta_J/10^{-6}cm^{-1}$	0.0002 (1)	0.002249 (1)
$\delta_K/10^{-6}$ cm^{-1}	0.00023 (3)	0.015793 (1)
N	15	560+15
d_{rms}/cm^{-1}	0.0000001	0.0000002
J_{max} for fit	6	50
J_{max} assigned	6	50
$K_{a\,max}$	3	19
$K_{c\,max}$	5	39

[a] Equilibrium rotational constants (A_e, B_e, C_e) from vibrational perturbation theory (t.w.) and experimental ground state rotational constants (A_0, B_0, C_0) from our present GHz and FTIR experiments. (t.w.) (''semi-experimental'' values). [b] This work including the lines of ref. 75.

5.2 Rovibrational analysis and parameters of the ν_{22} band of 1,2-dithiine

According to the calculated transition moments $\mu_b = -1.33 \times 10^{-3}$ D and $\mu_c = -2.20 \times 10^{-3}$ D the *b*-type absorption lines are predicted to have less than 40% of the strength of the corresponding *c*-type transitions. Around 1500 *b*-type transitions and around 4000 *c*-type transitions have been used in the adjustment. However, most of these *b*-type transitions, as already mentioned, are from non-split *c*-type and *b*-type transitions for $K_c \leq 11$ (around 1480 lines). Pure *b*-type transitions (around 20)

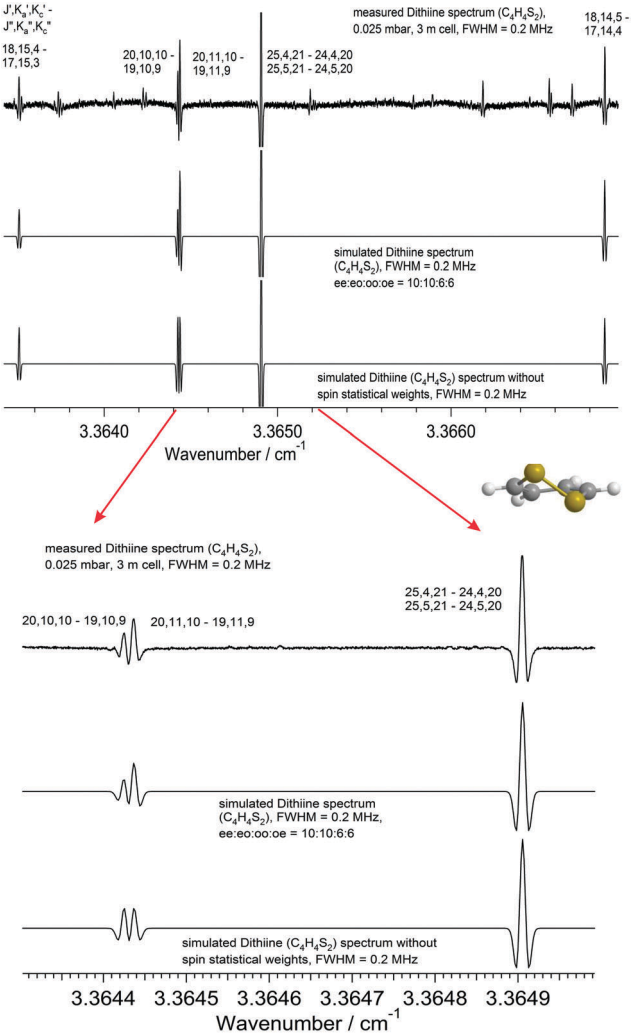

Fig. 10 A comparison of the *a*-type rotational transitions in the ground state of 1,2-dithiine measured at 295 K (top trace) with a simulation at 295 K (lower trace). The transitions between the lower J'', K_a'', K_c'' and the upper state J', K_a', K_c' are labeled as J', K_a', $K_c' \leftarrow J''$, K_a'', K_c''.

have been assigned and used near the center of the Q branch region. At higher J levels the *b*-type transitions are too weak to be detected. Pure *c*-type transitions (around 2500) have been assigned in the entire spectrum. In general, *b*- and *c*-type transitions up to $J \leq 78$, $K_a \leq 73$ and $K_c \leq 34$ were used for the fit of the spectroscopic constants. Global perturbations were observed, perhaps through interactions with the $2\nu_{23}$ state or $3\nu_{24}$ state or possibly also a combination with ν_{13} and even ν_{12}. The "polyad" between 600 and 700 cm^{-1} comprises 8 levels. The constants of the ground state have been held fixed to the values in Table 8 and the constants of the ν_{22} have been adjusted using the least squares analysis. Due to the interactions some of the sextic constants could be determined for ν_{22} as Table 9 shows, although the corresponding spectroscopic parameters have an effective meaning only. Around 4000 transitions were used in the fit with a d_{rms} = 0.00026 cm^{-1}.

A comparison of the measured spectrum with the simulated spectrum calculated using the parameters listed in Tables 8 and 9 is

Table 9 Spectroscopic constants in cm^{-1} of the vibrational states ν_{17}, ν_{22} and ν_3 of dithiine in the *A*-reduction. If there are no uncertainties listed (in parentheses in terms of 1σ in units of the last digits), the parameter was fixed during the fit at the value indicated

	ν_{17}	ν_{22}	ν_3
$\tilde{\nu}_0$	1308.87327 (38)	623.093915 (25)	1544.900370 (51)
A	0.1110980 (30)	0.110782038 (46)	0.1110040 (57)
B	0.1033660 (24)	0.103339231 (78)	0.1032180 (47)
C	0.05857310 (19)	0.05848408 (11)	0.05849980 (16)
$\Delta_J/10^{-6}$	0.000690 (20)	−0.0081798 (81)	0.00910 (12)
$\Delta_{JK}/10^{-6}$	0.001400 (92)	0.03133 (31)	0.0090 (11)
$\Delta_K/10^{-6}$	−0.0005986	−0.01207 (24)	−0.0130 (27)
$\delta_J/10^{-6}$	0.0002249	−0.002719 (40)	0.0002248
$\delta_K/10^{-6}$	0.0015793	0.01488 (12)	0.0015792
$\Phi_J/10^{-12}$	—	−1.181 (14)	—
$\Phi_{JK}/10^{-12}$	—	1.410 (44)	—
$\Phi_K/10^{-12}$	—	−0.492 (30)	—
$\phi_J/10^{-12}$	—	−0.4683 (57)	—
$\phi_{JK}/10^{-12}$	—	0.218 (15)	—
$\phi_K/10^{-12}$	—	−0.421 (19)	—
N	1006	4056	875
d_{rms}/cm^{-1}	0.000137	0.00026	0.00025
J_{max} for fit	32	78	40
J_{max} assigned	32	78	40
$K_{a\,max}$	12	73	10
$K_{c\,max}$	30	33	40

shown in Fig. 11 and 12 for the R and Q branch regions. The upper panel of Fig. 11 shows the complete ν_{22} fundamental (upper trace) and a simulation (lower trace). The lower panel of Fig. 11 is an enlarged region of the measured R branch lines (upper trace). The lower traces show simulations with and without nuclear spin statistical weights. As the simulation illustrates the intensity effect due to nuclear spin statistical weights is not visible in this part of the spectrum. The agreement between the measured and the simulated spectra is of comparable quality in both cases. Differences are due to numerous hot band lines not shown in the simulation and the relatively high noise level in the experiment.

Only 20% of the molecules are in the ground state at 295 K, while 80% molecules generate hot bands. The Q branch region in Fig. 12 (upper trace) illustrates numerous hot bands. The determination of the band center is only possible through the use of a Loomis–Wood assignment program. The other two panels display an enlargement of the Q branch region. As one can see in the third panel there is a remarkably good agreement between the simulation and the experimental spectrum, considering the important hot band contributions. A partial rovibrational analysis was possible for one of the hot bands.

5.3 Rovibrational analysis and parameters of the ν_{17} band of 1,2-dithiine

As the *ab initio* calculations shown in Table 2 suggest, the ν_{17} band is of B symmetry which permits both *b*- and *c*-type transitions with an intensity ratio of approximately 8 : 1 according to the calculations. A total of 1006 transitions obeying *b*-type selection rules (eo–oe and ee–oo) were assigned and analysed in a least squares adjustment varying only the three rotational constants and five centrifugal distortion constants of ν_{17} with a d_{rms} = 0.00014 cm^{-1} but fixing the parameters for Δ_K, δ_k and δ_j to the ground state values. Although perturbations have been encountered from J = 32 onwards, there is

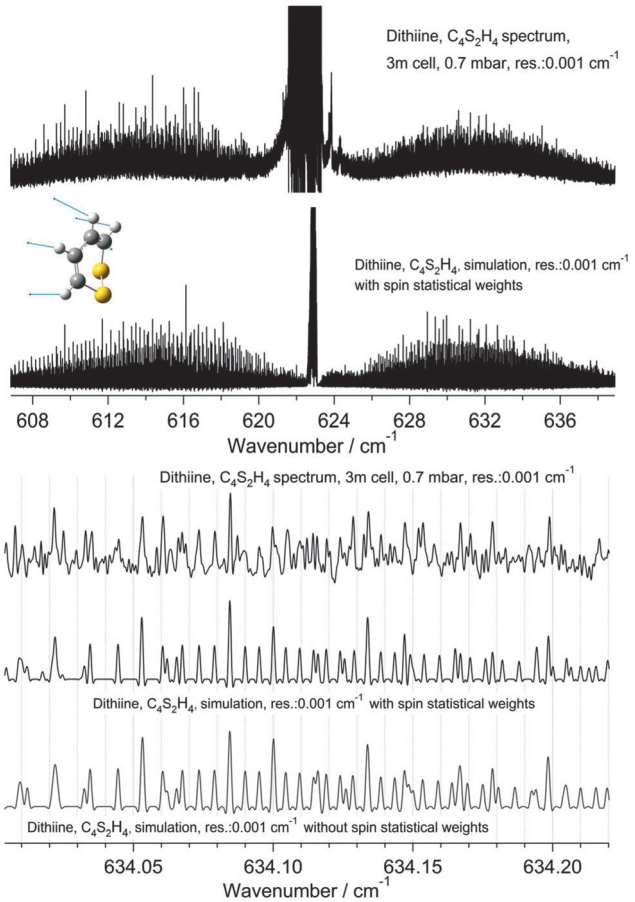

Fig. 11 A comparison of the ν_{22} band of 1,2-dithiine measured at 295 K (upper panel, top trace) with a simulation at 295 K (upper panel, lower trace). The upper trace in each panel displays the observed spectrum and the lower traces display the simulation with and without nuclear spin statistical weights. The middle and lower panels are enlargements of the sections of the R branches outlined in the upper panel. See parameters in the figure. The decadic absorbances $\lg(I_0/I)$ are shown as a function of wavenumber, with maximum peak values of $\lg(I_0/I)$ = 2.00 for the upper spectrum (cutoff of the Q-branch lines) and 0.7 for the lower spectrum (3 m path length, 0.7 mbar, $\Delta\tilde{\nu}$ = 0.001 cm^{-1}).

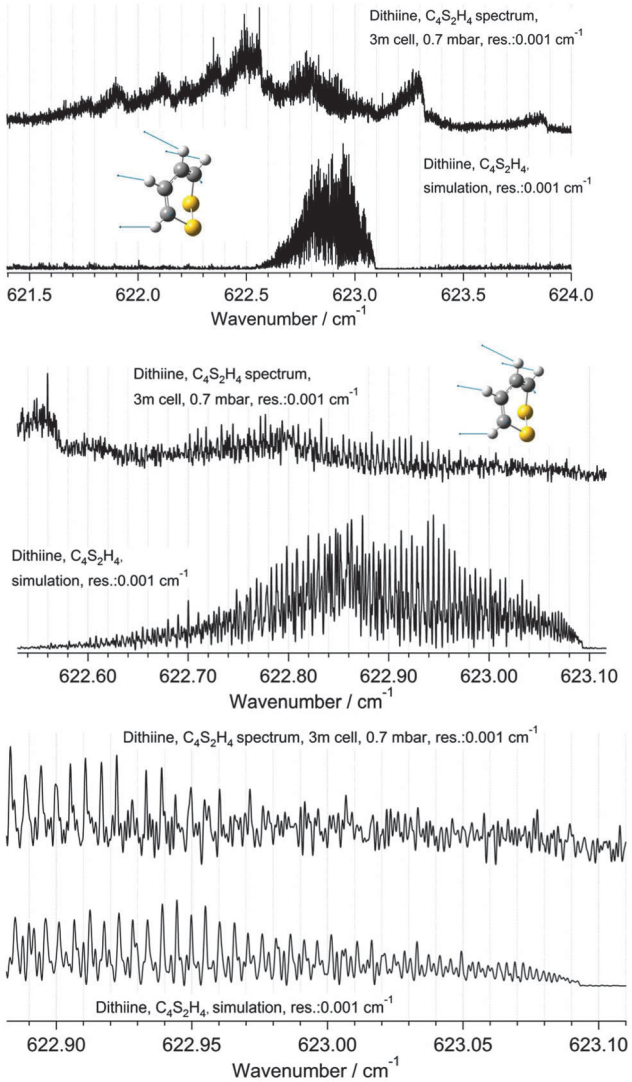

Fig. 12 A comparison of the Q branch region of the ν_{22} band of 1,2-dithiine measured at 295 K (upper panel, top trace) with simulation at 295 K (upper panel, lower trace). The upper trace in each panel displays the observed spectrum and the lower trace displays the simulation. The middle and lower panels are enlargements of the sections of the Q branches outlined in the upper panel. The numerous Q branches resulting from hot bands are visible in the experimental spectrum. See parameters in the figure. The decadic absorbances $\lg(I_0/I)$ are shown as a function of wavenumber, with maximum peak values of $\lg(I_0/I)$ = 1.20 for the upper and middle spectra (cutoff of the Q-branch lines) and 0.7 for the lower spectrum (3 m path length, 0.7 mbar, $\Delta\tilde{\nu}$ = 0.001 cm^{-1}).

good agreement between the simulated spectrum based on the parameters shown in Table 9 and the observed spectra as shown in Fig. 13. Only unperturbed lines up to $J \leq 32$ have been used in the least squares adjustment. However, the assignment of the perturbed lines above $J > 32$ has been checked by ground state combination differences calculated from the perturbed P and R branch lines of ν_{17}.

The strong Q branch as shown in Fig. 13 with a calculated $|\mu_b/\mu_c|$ = 2.8 is due to *c*-type transitions according to the prediction. However, the Q branch region is more complicated due to numerous hot bands. It was not possible to identify single *c*-type transitions because of the strong congestion of lines which is in agreement with the predicted transitions. Some of the hot band lines can be grouped into series using the Loomis–Wood diagram, however an adjustment of the spectroscopic parameters is not yet possible. Considering a possible assignment of the band observed at 1308.9 cm^{-1} to ν_4 predicted at 1350 cm^{-1} by the *ab initio* calculations reported in Table 2, we have also conducted an analysis using *a*-type selection rules in the assignment. While this assignment gives a satisfactory fit as well, the shape of the Q branch in the simulation is much broader and differs significantly from the experimental shape. Therefore the assignment as ν_{17} seems to be well justified. As in the case of ν_{22}, our data are insufficient to make use of nuclear spin statistical weights in the assignment of ν_{17}. We have also tested fits with a variation of Δ_K (and also other parameters) being systematically fixed at a series of values. The conclusion from these tests is that the shape of the Q branch

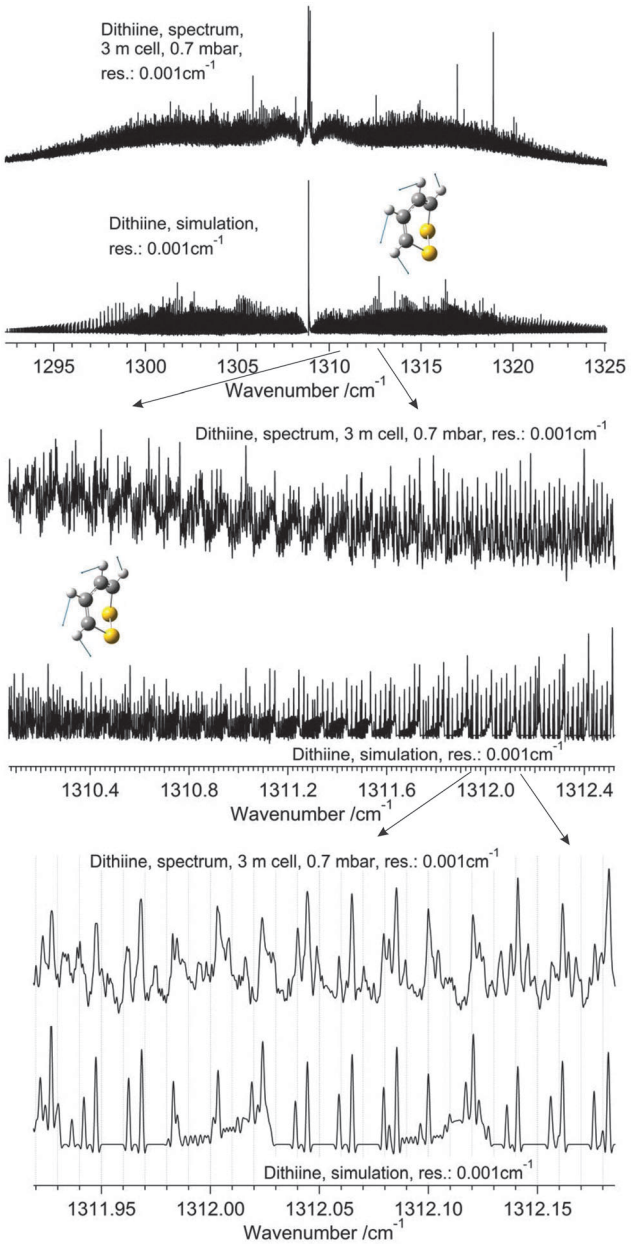

Fig. 13 A comparison of the ν_{17} band of 1,2-dithiine measured at 295 K (upper panel, top trace) with a simulation at 295 K (upper panel, lower trace). The upper trace in each panel displays the observed spectrum and the lower trace displays the simulation. The middle and lower panels are enlargements of the sections of the R branches outlined in the upper panel. The Q branch region consists of numerous Q branches resulting from hot bands. See parameters in the figure. The decadic absorbances $\lg(I_0/I)$ are shown as a function of wavenumber, with maximum peak values of $\lg(I_0/I)$ = 1.60 for the upper spectrum (cutoff of the Q-branch lines) and 0.6 for the two lower panels.

can be best simulated if all quartic constants are fixed at the values of the quartic constants of the ground state. However, this fixing leads to slightly larger d_{rms} = 0.0005 cm^{-1} which is still below the instrumental resolution. Thus the spectroscopic parameters have clearly a meaning as "effective parameters" only which it does, however, not affect our conclusions.

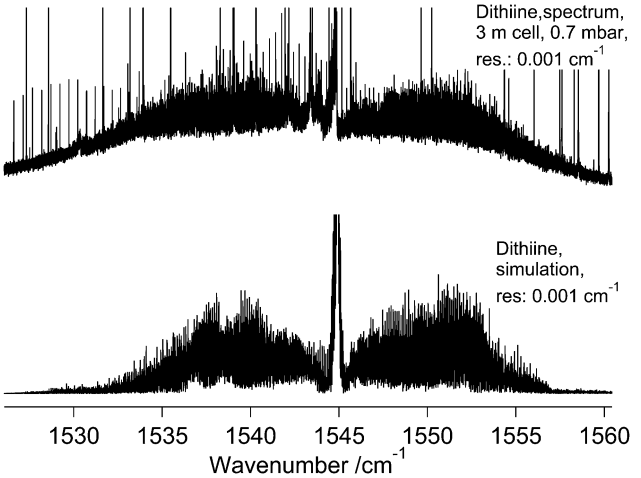

Fig. 14 A comparison of the ν_3 band of 1,2-dithiine consisting of *a*-type transitions measured at 295 K (top trace) with a simulation at 295 K (lower trace). The upper trace displays the observed spectrum and the lower trace displays the simulation. See parameters in the figure. The decadic absorbances $\lg(I_0/I)$ are shown as a function of wavenumber, with the maximum peak values of $\lg(I_0/I)$ = 0.3 for the spectrum (cutoff of the Q-branch lines).

5.4 Rovibrational analysis and parameters of the ν_3 band of 1,2-dithiine

Consistent with A symmetry under C_2, 875 transitions from the ν_3 band were assigned obeying *a*-type selection rules eo–ee and oe–oo (Fig. 14). These lines were fit with the variation of one more spectroscopic constant than used for the ν_{17} band. To minimize the possible effects from the observed perturbation in this band, only transitions with J(max) = 40 (onset of local resonances) were assigned. There is good agreement between the observed and simulated spectra in unperturbed regions and the band provides a good example for a totally symmetric fundamental.

6 Discussion and conclusions

Designing and selecting molecules towards specific properties for a variety of applications is a well-known task in chemistry.[133,134] The theoretical selection and spectroscopic characterization of a chiral molecule suitable for the measurement of the parity violating energy difference $\Delta_{\mathrm{pv}}E$ between the enantiomers by the method proposed by us three decades ago[52] is a new, very great challenge, given the current technical possibilities.[70] The present work contributes some major results towards this goal, both theoretical and spectroscopic, for the moderately complex molecule 1,2-dithiine.

From the theoretical point of view, we have shown that in the ground and low energy rovibrational states parity violation clearly dominates over tunneling in the quantum dynamics of 1,2-dithiine by many orders of magnitude. Thus the reaction enthalpy $\Delta_{\mathrm{pv}}H_0$ for the stereomutation reaction (1) is, in principle, a measurable quantity for 1,2-dithiine, similar to the simpler molecule dichlorodisulfane (Cl–SS–Cl) which we had studied before,[71] and quite different from the case of disulfane HSSH.[72] A detailed study of the conformation dependence of

parity violation in 1,2-dithiine, indeed, shows that this is a particularly favorable molecule, as the maximum of the absolute value of the parity violating potential (about 6×10^{-12} (hc) cm^{-1} corresponding to $\Delta_{pv}E^{el}(q_{max}) = 12 \times 10^{-12}$ (hc) cm^{-1} in Fig. 4) is found to be close to the equilibrium geometry. The expectation value $\Delta_{pv}E_0$ in the vibrational ground state has been calculated approximately by means of the ground state of the lowest quasiadiabatic channel for torsion and differs by less than 10% from the equilibrium value $\Delta_{pv}E^{el}(q_e) = 11.44 \times 10^{-12}$ (hc) cm^{-1} (eqn (4)), very close to the maximum value. Again, 1,2-dithiine might be compared to ClSSCl in this respect where the predicted $\Delta_{pv}E_0$ is smaller by a factor of about 8 (1.35×10^{-12} (hc) cm^{-1} [71]), because of the relatively unfavorable position of the equilibrium geometry, far removed from the position of the maximum in the parity violating potential as a function of torsional angle with $\Delta_{pv}E^{el}(q_{max}) \approx 12 \times 10^{-12}$ (hc) cm^{-1}, which is actually quite similar to the maximum value in 1,2-dithiine. Also in our recent study of $\Delta_{pv}E$ in trisulfane, the predicted $\Delta_{pv}E_0 = 1.6 \times 10^{-12}$ (hc) cm^{-1} is found to be much smaller than the maximum value as a function of the torsional (stereomutation reaction) coordinate ($\Delta_{pv}E^{el}(q_{max}) = 8.2 \times 10^{-12}$ (hc) cm^{-1}). Another, even less favorable example of this kind, which we encountered in the past, is 1,3-difluoroallene which in many other spectroscopic aspects is quite easily accessible.[76]

Our theoretical results also provide further evidence that simple scaling laws, as repeatedly discussed since the early theoretical work of Bouchiat and Bouchiat[62,63] for atoms (with parity violating effects increasing with about the third power of the atomic number Z), are of limited significance in predicting parity violation in molecules. Many earlier discussions have pointed out that an approximate scaling with Z^5 can be derived for parity violation in molecules[31,35,37,61,83] with the implicit assumption that the number of neutrons in a typical nucleus is proportional to Z as well. However, the strong dependence of molecular parity violation upon conformation can easily change the effects by an order of magnitude and more, as seen from the examples given above. Examples are known, where a conformation change in a substituent without changing the stereomutation coordinate can even change the sign of the parity violating potential without changing the enantiomeric nature.[33,35,135] Indeed, in strong contrast to atomic parity violation the molecular parity violation is characterized by a complicated $(3N - 6)$-dimensional effective parity violating potential hypersurface to be added to the ordinary parity conserving potential hypersurface as a perturbation of different symmetry,[9,61] and our results of 1,2-dithiine in relation to other molecules studied demonstrate the complicated consequences of this. It has been pointed out[61] that a Z^n scaling might be applied to a series of homologous molecules either at their individual equilibrium geometries or at identical (non-equilibrium) geometries or else at geometries related to the maximum absolute values of $|\Delta_{pv}E^{el}|$ of the different molecules, with quite different results in each case. As an alternative to the effective parity violating potential one might also consider the tensor components of the parity violating potential[61] or values corresponding to the main chiral axes[36] in relation to a Z^n scaling. In practice, simple rules including Z^n-scaling and geometrical factors might be derived as the first selection criteria,[48] but in the end, for individual molecules to be selected for the very demanding experiments, quantitative calculations as carried out here for 1,2-dithiine including the conformation dependence and tunneling processes are required. In this respect, 1,2-dithiine turns out to be quite a favorable candidate for experiments.

Tunneling in the ground state has been shown in the present work to be completely suppressed for 1,2-dithiine with

$$\Delta E_{\pm} < 10^{-24}\ (hc)\ cm^{-1} \ll \Delta E_{pv} \simeq 10^{-11}\ (hc)\ cm^{-1} \qquad (6)$$

similar to ClSSCl, for example.[71] However the barrier for stereomutation in 1,2-dithiine is much lower than in ClSSCl. Thus in 1,2-dithiine tunneling can become important above about 2300 cm^{-1}, making states of well-defined parity accessible in the infrared range, where powerful high resolution lasers are available for parity selection experiments[70] and where spectroscopic analyses are possible, making the ''infrared route'' towards parity violation possible. This does not exclude the possibility of also using the route *via* excited electronic states possibly with rovibrational preselection, as suggested for 1,3-difluoroallene,[76] but too little is known at present concerning the high resolution electronic spectra of 1,2-dithiine for which we plan a more detailed study as well.

We have shown here that high resolution analyses are possible in the infrared range for 1,2-dithiine, with three strong fundamentals ν_{22} at 623.094 cm^{-1}, ν_3 at 1544.900 cm^{-1} and ν_{17} at 1308.873 cm^{-1}. The latter band might be used as a starting point for a stepwise two-photon excitation to the $2\nu_{17}$ range at 2600 cm^{-1}, where tunneling can be important, if couplings to tunneling sublevels of well-defined parity can be identified. In the future also high resolution analyses of the $2\nu_{17}$ absorptions or the CH stretching polyad at around 3000 cm^{-1} can become possible. Indeed, the overtone of the fundamental ν_3 studied here is predicted to show a strong Fermi-resonance with the CH-stretching fundamentals using our *ab initio* calculations. In all cases a major remaining challenge will be the analysis of rovibrational couplings to tunneling sublevels of well-defined parity. Some first evidence for rovibrational couplings has been seen in the present analysis of ν_{17}. At higher energies intramolecular rovibrational couplings are very likely,[119] given the high density of vibrational states, which is about 50 states per cm^{-1} interval at 2600 cm^{-1} and 1300 states per cm^{-1} interval at around 3000 cm^{-1}. The corresponding spectroscopic analyses of the resulting complex spectra can be successful, however, with existing high resolution infrared laser spectroscopy of molecular beams, achieving even hyperfine resolution in excited vibrational states of ammonia, for example, (*i.e.* $\Delta\nu < 1$ MHz around $\nu = 100$ THz or $\Delta\tilde{\nu} < 0.00003$ cm^{-1} at $\tilde{\nu} = 3300$ cm^{-1} [70]). Double resonance with IR-lasers[70] and GHz spectroscopy[103] can also be helpful in this context. We have furthermore carried out extensive calculations on various deuterated isotopomers of 1,2-dithiine, where the CD infrared chromophore makes the wavenumber range just above the tunneling switching range accessible. These results are presented in the ESI† as well.

The study of the lowest frequency fundamentals by synchrotron-based THz (FTIR) spectroscopy is in progress.

The present work thus clearly opens the route towards successful spectroscopic experiments to measure the parity violating energy difference $\Delta_{pv}E$ in 1,2-dithiine with a rather short time τ_{pv} = 1.5 s for complete parity change in this molecule; the initial time evolution in the ms range would be clearly detectable by the now available techniques.[70] While a simpler molecule with fewer atoms would certainly still be desirable to complete the necessary spectroscopic groundwork, 1,2-dithiine has the advantage of a relatively rigid structure apart from the simple spin 1/2 protons with only the rather light C and S nuclei with zero spin, a simple nuclear structure, which is almost ideal for highly accurate theoretical analyses in terms of fundamental parameters of the standard model of particle physics from experimental results, once available.[9]

Acknowledgements

Our work is financially supported by an advanced grant from the ERC, the Schweizerischer Nationalfonds and the ETH Zürich. The research leading to these results had in particular also received funding from the European Union's Seventh Framework Programme (FP7/2007–20013) ERC grant agreement no. 290925. Very substantial help from Guido Grassi and Fabienne Arn in the synthesis work is gratefully acknowledged. We also acknowledge the help from and enjoyed the discussion with Andreas Schneider and Andres Laso and also support from the COST project MOLIM.

References

1 J. H. van't Hoff, *La chimie dans l'espace*, P. M. Bazendijk, Rotterdam, 1887, reprinted with commentary in ref. 2.
2 C. Bourgois, *Louis Pasteur, J. H. van't Hoff, A. Werner: sur la dissymétrie moléculaire*, Collection Epistème, Dôle, France, 1986.
3 J. H. van't Hoff, *Vorlesungen über theoretische und physikalische Chemie, Heft 2. Die chemische Statik*, Vieweg, Braunschweig, 1899.
4 E. Fischer, *Ber. Dtsch. Chem. Ges.*, 1894, **27**, 2985–2993.
5 V. Prelog, Chirality in Chemistry, in *Les prix Nobel 1975, Nobel Lectures*, Elsevier, New York, ch. Chemistry, 1971–1980, pp. 203–216 (the Nobel Foundation 1975).
6 M. Quack, *Eur. Rev.*, 2014, **22**, S50–S86.
7 F. Hund, *Z. Phys.*, 1927, **43**, 805–826.
8 F. Merkt and M. Quack, Molecular Quantum Mechanics and Molecular Spectra, Molecular Symmetry, and Interaction of Matter with Radiation, *Handbook of High-Resolution Spectroscopy*, John Wiley & Sons, Ltd, Chichester, 2011, ch. 1, vol. 1, pp. 1–55.
9 M. Quack, Fundamental Symmetries and Symmetry Violations from High Resolution Spectroscopy, *Handbook of High Resolution Spectroscopy*, John Wiley & Sons, Ltd, Chichester, New York, 2011, ch. 18, vol. 1, pp. 659–722.
10 M. Quack, *Angew. Chem., Int. Ed. Engl.*, 1989, **28**, 571–586.
11 T. Lee and C. Yang, *Phys. Rev.*, 1956, **104**, 254–258.
12 C. Wu, E. Ambler, R. Hayward, D. Hoppes and R. Hudson, *Phys. Rev.*, 1957, **105**, 1413–1415.
13 J. I. Friedman and V. L. Telegdi, *Phys. Rev.*, 1957, **105**, 1681–1682.
14 R. L. Garwin, L. M. Lederman and M. Weinrich, *Phys. Rev.*, 1957, **105**, 1415–1417.
15 H. Schopper, *Philos. Mag.*, 1957, **2**, 710–713.
16 H. Schopper, *Naturwissenschaften*, 1958, **45**, 453–456.
17 S. L. Glashow, *Nucl. Phys.*, 1961, **22**, 579–588.
18 S. Weinberg, *Phys. Rev. Lett.*, 1967, **19**, 1264–1266.
19 A. Salam, in *Weak and electromagnetic interactions*, ed. N. Svartholm, Almkvist & Wiksell, Stockholm, 1968, pp. 367–377.
20 M. J. G. Veltman, *Rev. Mod. Phys.*, 2000, **72**, 341–349.
21 G. 't Hooft, *Rev. Mod. Phys.*, 2000, **72**, 333–339.
22 Y. Yamagata, *J. Theor. Biol.*, 1966, **11**, 495–498.
23 D. W. Rein, *J. Mol. Evol.*, 1974, **4**, 15–22.
24 S. F. Mason, *Chemical Evolution: Origin of the Elements, Molecules, and Living Systems*, Clarendon Press, Oxford, 1991.
25 P. Frank, W. Bonner and R. N. Zare, in *On the one hand but not on the other: the challenge of the origin and survival of homochirality in prebiotic chemistry*, ed. E. Keinan and I. Schechter, Wiley-VCH, Weinheim, 2001, book section 11, pp. 175–208.
26 M. Quack, *Angew. Chem., Int. Ed.*, 2002, **41**, 4618–4630.
27 M. Quack, *Chimia*, 2003, **57**, 147–160.
28 J. Jortner, *Philos. Trans. R. Soc. London, Ser. B*, 2006, **361**, 1877–1891.
29 M. Quack, *Adv. Chem. Phys.*, 2014, **157**, 249–290.
30 V. S. Letokhov, *Phys. Lett. A*, 1975, **53**, 275–276.
31 R. A. Hegström, D. W. Rein and P. G. H. Sandars, *J. Chem. Phys.*, 1980, **73**, 2329–2341.
32 S. F. Mason and G. E. Tranter, *Mol. Phys.*, 1984, **53**, 1091–1111.
33 A. Bakasov, T.-K. Ha and M. Quack, Proc. of the 4th Trieste Conference (1995), Chemical Evolution: Physics of the Origin and Evolution of Life, ed. J. Chela Flores and F. Rolin, Kluwer, Dordrecht, 1996, pp. 287–296.
34 P. Lazzeretti and R. Zanasi, *Chem. Phys. Lett.*, 1997, **279**, 349–354.
35 A. Bakasov, T. K. Ha and M. Quack, *J. Chem. Phys.*, 1998, **109**, 7263–7285.
36 A. Bakasov and M. Quack, *Chem. Phys. Lett.*, 1999, **303**, 547–557.
37 J. K. Laerdahl and P. Schwerdtfeger, *Phys. Rev. A: At., Mol., Opt. Phys.*, 1999, **60**, 4439–4453.
38 R. Berger and M. Quack, *J. Chem. Phys.*, 2000, **112**, 3148–3158.
39 M. Quack and J. Stohner, *Phys. Rev. Lett.*, 2000, **84**, 3807–3810.
40 J. K. Laerdahl, P. Schwerdtfeger and H. M. Quiney, *Phys. Rev. Lett.*, 2000, **84**, 3811–3814.
41 M. Quack and J. Stohner, *Z. Phys. Chem.*, 2000, **214**, 675–703.
42 M. Quack and J. Stohner, *J. Chem. Phys.*, 2003, **119**, 11228–11240.

43 A. C. Hennum, T. Helgaker and W. Klopper, *Chem. Phys. Lett.*, 2002, **354**, 274–282.
44 L. Horný and M. Quack, *Mol. Phys.*, 2015, **113**, 1768–1779.
45 M. Quack and J. Stohner, *Chirality*, 2001, **13**, 745–753.
46 R. Berger, in *Parity-violation effects in molecules, in Relativistic Electronic Structure Theory*, ed. P. Schwerdtfeger, Elsevier, Amsterdam, 2004, part 2, book section 4, pp. 188–288.
47 M. Quack and J. Stohner, *Chimia*, 2005, **59**, 530–538.
48 M. Quack, J. Stohner and M. Willeke, *Annu. Rev. Phys. Chem.*, 2008, **59**, 741–769.
49 O. N. Kompanets, A. R. Kukudzhanov, V. S. Letokhov and L. L. Gervits, *Opt. Commun.*, 1976, **19**, 414–416.
50 E. Arimondo, P. Glorieux and T. Oka, *Opt. Commun.*, 1977, **23**, 369–372.
51 R. A. Harris and L. Stodolsky, *Phys. Lett. B*, 1978, **78**, 313–317.
52 M. Quack, *Chem. Phys. Lett.*, 1986, **132**, 147–153.
53 M. J. M. Pepper, I. Shavitt, P. v. Ragué Schleyer, M. N. Glukhovtsev, R. Janoschek and M. Quack, *J. Comput. Chem.*, 1995, **16**, 207–225.
54 B. Darquié, C. Stoeffler, A. Shelkovnikov, C. Daussy, A. Amy-Klein, C. Chardonnet, S. Zrig, L. Guy, J. Crassous, P. Soulard, P. Asselin, T. R. Huet, P. Schwerdtfeger, R. Bast and T. Saue, *Chirality*, 2010, **22**, 870–884.
55 M. Quack, *Faraday Discuss.*, 2011, **150**, 533–565.
56 M. Quack, *Faraday Discuss.*, 2011, **150**, 123–127.
57 A. Bauder, A. Beil, D. Luckhaus, F. Müller and M. Quack, *J. Chem. Phys.*, 1997, **106**, 7558–7570.
58 C. Daussy, T. Marrel, A. Amy-Klein, C. T. Nguyen, C. J. Bordé and C. Chardonnet, *Phys. Rev. Lett.*, 1999, **83**, 1554–1557.
59 M. Schnell and J. Küpper, *Faraday Discuss.*, 2011, **150**, 1–17.
60 S. K. Tokunaga, C. Stoeffler, F. Auguste, A. Shelkovnikov, C. Daussy, A. Amy-Klein, C. Chardonnet and B. Darquié, *Mol. Phys.*, 2013, **111**, 2363–2373.
61 A. Bakasov, R. Berger, T.-K. Ha and M. Quack, *Int. J. Quantum Chem.*, 2004, **98**, 393–407.
62 M. A. Bouchiat and C. Bouchiat, *J. Phys.*, 1974, **35**, 899–927.
63 M. A. Bouchiat and C. Bouchiat, *J. Phys.*, 1975, **36**, 493–509.
64 R. Conti, P. Bucksbaum, S. Chu, E. Commins and L. Hunter, *Phys. Rev. Lett.*, 1979, **42**, 343–346.
65 S. C. Bennett and C. E. Wieman, *Phys. Rev. Lett.*, 1999, **82**, 2484–2487.
66 V. M. Shabaev, K. Pachucki, I. Tupitsyn and V. A. Yerokhin, *Phys. Rev. Lett.*, 2005, **94**, 213002.
67 K. Tsigutkin, D. Dounas-Frazer, A. Family, J. E. Stalnaker, V. V. Yashchuk and D. Budker, *Phys. Rev. Lett.*, 2009, **103**, 071.
68 R. Prentner, M. Quack, J. Stohner and M. Willeke, *J. Phys. Chem. A*, 2015, **119**, 12805–12822.
69 M. Quack and M. Willeke, *J. Phys. Chem. A*, 2006, **110**, 3338–3348.
70 P. Dietiker, E. Miloglyadov, M. Quack, A. Schneider and G. Seyfang, *J. Chem. Phys.*, 2015, **143**, 244305.
71 R. Berger, M. Gottselig, M. Quack and M. Willeke, *Angew. Chem., Int. Ed.*, 2001, **40**, 4195–4198.
72 M. Gottselig, D. Luckhaus, M. Quack, J. Stohner and M. Willeke, *Helv. Chim. Acta*, 2001, **84**, 1846–1861.
73 M. J. Frisch, G. W. Trucks, H. B. Schlegel, G. E. Scuseria, M. A. Robb, J. R. Cheeseman, G. Scalmani, V. Barone, B. Mennucci, G. A. Petersson, H. Nakatsuji, M. Caricato, X. Li, H. P. Hratchian, A. F. Izmaylov, J. Bloino, G. Zheng, J. L. Sonnenberg, M. Hada, M. Ehara, K. Toyota, R. Fukuda, J. Hasegawa, M. Ishida, T. Nakajima, Y. Honda, O. Kitao, H. Nakai, T. Vreven, J. A. Montgomery, Jr., J. E. Peralta, F. Ogliaro, M. Bearpark, J. J. Heyd, E. Brothers, K. N. Kudin, V. N. Staroverov, R. Kobayashi, J. Normand, K. Raghavachari, A. Rendell, J. C. Burant, S. S. Iyengar, J. Tomasi, M. Cossi, N. Rega, J. M. Millam, M. Klene, J. E. Knox, J. B. Cross, V. Bakken, C. Adamo, J. Jaramillo, R. Gomperts, R. E. Stratmann, O. Yazyev, A. J. Austin, R. Cammi, C. Pomelli, J. W. Ochterski, R. L. Martin, K. Morokuma, V. G. Zakrzewski, G. A. Voth, P. Salvador, J. J. Dannenberg, S. Dapprich, A. D. Daniels, Ö. Farkas, J. B. Foresman, J. V. Ortiz, J. Cioslowski and D. J. Fox, *Gaussian 09 Revision E.01*, Gaussian Inc., Wallingford, CT, 2009.
74 H.-J. Werner, P. J. Knowles, G. Knizia, F. R. Manby and M. Schütz, *Wiley Interdiscip. Rev.: Comput. Mol. Sci.*, 2012, **2**, 242–253.
75 J. Z. Gillies, C. W. Gillies, E. A. Cotter, E. Block and R. DeOrazio, *J. Mol. Spectrosc.*, 1996, **180**, 139–144.
76 M. Gottselig and M. Quack, *J. Chem. Phys.*, 2005, **123**, 084305.
77 W. Schroth, F. Billig and H. Langguth, *Z. Chem.*, 1965, **5**, 353–354.
78 W. Schroth, F. Billig and G. Reinhold, *Angew. Chem., Int. Ed.*, 1967, **6**, 698–699.
79 F. Bohlmann and K.-M. Kleine, *Chem. Ber.*, 1965, **98**, 3081–3086.
80 J. T. Mortensen, J. S. Sørensen and N. A. Sørensen, *Acta Chem. Scand.*, 1965, **18**, 2392–2394.
81 E. Block, M. Birringer, R. DeOrazio, J. Fabian, R. S. Glass, C. Guo, C. He, E. Lorance, Q. Qian, T. B. Schroeder, Z. Shan, M. Thiruvazhi, G. S. Wilson and X. Zhang, *J. Am. Chem. Soc.*, 2000, **122**, 5052–5064.
82 E. Block, *Phosphorus, Sulfur Silicon Relat. Elem.*, 1999, **153**, 173–192.
83 S. Pelloni, F. Faglioni and P. Lazzeretti, *Mol. Phys.*, 2013, **111**, 2387–2391.
84 S. Pelloni, F. Faglioni, A. Soncini, A. Ligabue and P. Lazzeretti, *Chem. Phys. Lett.*, 2003, **375**, 583–590.
85 A. Soncini, F. Faglioni and P. Lazzeretti, *Phys. Rev. A: At., Mol., Opt. Phys.*, 2003, **68**, 033402.
86 J. Fabian and P. Birner, *Collect. Czech. Chem. Commun.*, 1988, **53**, 2096–2115.
87 R. S. Glass, N. E. Gruhn, D. L. Lichtenberger, E. Lorance, J. R. Pollard, M. Birringer, E. Block, R. DeOrazio, C. He, Z. Shan and X. Zhang, *J. Am. Chem. Soc.*, 2000, **122**, 5065–5074.
88 J. V. Ortiz, *J. Phys. Chem. A*, 2002, **106**, 5924–5927.
89 J. Fabian, M. Mann and M. Petiau, *Molecular Modeling Annual*, 2000, **6**, 177–185.

90 C. Fábri, L. Horný and M. Quack, *ChemPhysChem*, 2015, **16**, 3584–3589.
91 S. Albert, K. Keppler, P. Lerch, M. Quack and A. Wokaun, *J. Mol. Spectrosc.*, 2015, **315**, 92–101.
92 S. Albert, I. Bolotova, Z. Chen, C. Fábri, L. Horný, M. Quack, G. Seyfang and D. Zindel, *Chimia*, 2015, Proceedings of the Swiss Chemical Society Fall meeting 2015, **69**, PC105.
93 S. Albert, I. Bolotova, Z. Chen, C. Fábri, L. Horný, M. Quack, G. Seyfang and D. Zindel, *Proceedings of QAMTS 2015*, Beatenberg, Switzerland, 2015, P. 10.
94 S. Albert, I. Bolotova, Z. Chen, C. Fábri, L. Horný, M. Quack, G. Seyfang and D. Zindel, Proceedings of the 20th Symposium on Atomic, Cluster and Surface Physics (SASP 2016), Davos, Switzerland, February 7–12, 2016, Innsbruck, 2016, pp. 127–130, ISBN: 978-3-903122-04-8.
95 H.-J. Werner, P. J. Knowles, G. Knizia, F. R. Manby and M. Schütz, *Wiley Interdiscip. Rev.: Comput. Mol. Sci.*, 2012, **2**, 242–253.
96 H.-J. Werner, P. J. Knowles, G. Knizia, F. R. Manby, M. Schütz, P. Celani, T. Korona, R. Lindh, A. Mitrushenkov, G. Rauhut, K. R. Shamasundar, T. B. Adler, R. D. Amos, A. Bernhardsson, A. Berning, D. L. Cooper, M. J. O. Deegan, A. J. Dobbyn, F. Eckert, E. Goll, C. Hampel, A. Hesselmann, G. Hetzer, T. Hrenar, G. Jansen, C. Köppl, Y. Liu, A. W. Lloyd, R. A. Mata, A. J. May, S. J. McNicholas, W. Meyer, M. E. Mura, A. Nicklass, D. P. O'Neill, P. Palmieri, D. Peng, K. Pflüger, R. Pitzer, M. Reiher, T. Shiozaki, H. Stoll, A. J. Stone, R. Tarroni, T. Thorsteinsson and M. Wang, *MOLPRO, version 2012.1, a package of ab initio programs*, 2012, see http://www.molpro.net.
97 L. Horný and M. Quack, *Faraday Discuss. Chem. Soc.*, 2011, **150**, 152–154.
98 T. D. Crawford, C. D. Sherrill, E. F. Valeev, J. T. Fermann, R. A. King, M. L. Leininger, S. T. Brown, C. L. Janssen, E. T. Seidl, J. P. Kenny and W. D. Allen, *J. Comput. Chem.*, 2007, **28**, 1610–1616.
99 B. Fehrensen, D. Luckhaus and M. Quack, *Z. Phys. Chem.*, 1999, **209**, 1–19.
100 B. Fehrensen, D. Luckhaus and M. Quack, *Chem. Phys. Lett.*, 1999, **300**, 312–320.
101 B. Fehrensen, D. Luckhaus and M. Quack, *Chem. Phys.*, 2007, **338**, 90–105.
102 R. Xu, W. B. Schweizer and H. Frauenrath, *Chem. – Eur. J.*, 2009, **15**, 9105–9116.
103 M. Suter and M. Quack, *Appl. Opt.*, 2015, **54**, 4417–4431.
104 A. Maki and J. S. Wells, *Wavenumber Calibration Tables from Heterodyne Frequency Measurements*, NIST Special Publication 821, USA, 1991.
105 L. S. Rothman, I. E. Gordon, A. Barbe, D. C. Benner, P. F. Bernath, M. Birk, V. Boudon, L. R. Brown, A. Campargue, J. P. Champion, K. Chance, L. H. Coudert, V. Dana, V. M. Devi, S. Fally, J. M. Flaud, R. R. Gamache, A. Goldman, D. Jacquemart, I. Kleiner, N. Lacome, W. J. Lafferty, J. Y. Mandin, S. T. Massie, S. N. Mikhailenko, C. E. Miller, N. Moazzen-Ahmadi, O. V. Naumenko, A. V. Nikitin, J. Orphal, V. I. Perevalov, A. Perrin, A. Predoi-Cross, C. P. Rinsland, M. Rotger, M. Šimecková, M. A. H. Smith, K. Sung, S. A. Tashkun, J. Tennyson, R. A. Toth, A. C. Vandaele and J. Vander Auwera, *J. Quant. Spectrosc. Radiat. Transfer*, 2009, **110**, 533–572.
106 S. Albert, K. Keppler Albert and M. Quack, *Trends Opt. Photonics*, 2003, **84**, 177–180.
107 S. Albert and M. Quack, *ChemPhysChem*, 2007, **8**, 1271–1281.
108 S. Albert, S. Bauerecker, M. Quack and A. Steinlin, *Mol. Phys.*, 2007, **105**, 541–558.
109 S. Albert, K. Keppler Albert and M. Quack, High Resolution Fourier Transform Infrared Spectroscopy, *Handbook of High Resolution Spectroscopy*, John Wiley & Sons, Ltd, 2011, ch. 26, vol. 2, pp. 965–1019.
110 M. Quack, *Mol. Phys.*, 1977, **34**, 477–504.
111 K. v. Puttkamer and M. Quack, *Mol. Phys.*, 1987, **62**, 1047–1064.
112 K. v. Puttkamer, M. Quack and M. A. Suhm, *Mol. Phys.*, 1988, **65**, 1025–1045.
113 E. Riedle, A. Beil, D. Luckhaus and M. Quack, *Mol. Phys.*, 1994, **81**, 1–15.
114 H. C. Longuet-Higgins, *Mol. Phys.*, 1963, **6**, 445–460.
115 C. M. Western, *PGOPHER, a Program for Simulating Rotational Structure!*, University of Bristol Research Data Repository, Bristol, 2014.
116 C. M. Western, *Handbook of High-Resolution Spectroscopy*, John Wiley &, Ltd, Chichester, 2011, ch. 1, vol. 2, pp. 1415–1435.
117 D. Luckhaus and M. Quack, *Mol. Phys.*, 1989, **68**, 745–758.
118 B. P. Winnewisser, J. Reinstädtler, K. M. T. Yamada and J. Behrend, *J. Mol. Spectrosc.*, 1989, **136**, 12–18.
119 S. Albert, K. Keppler Albert, H. Hollenstein, C. Manca Tanner and M. Quack, Fundamentals of Rotation-Vibration Spectra, *Handbook of High-Resolution Spectroscopy*, John Wiley & Sons, Ltd, Chichester, 2011, ch. 3, vol. 1, pp. 117–173.
120 S. Albert, M. Winnewisser and B. P. Winnewissser, *Ber. Bunsenges. Phys. Chem.*, 1996, **100**, 1876–1896.
121 S. Albert, M. Winnewisser and B. P. Winnewissser, *Microchim. Acta*, 1997, **14**, 79–88.
122 S. Albert, K. Albert, M. Winnewisser and B. P. Winnewissser, *Ber. Bunsenges. Phys. Chem.*, 1998, **102**, 1428–1448.
123 S. Albert, H. Hollenstein, M. Quack and M. Willeke, *Mol. Phys.*, 2004, **102**, 1671–1686.
124 S. Albert, H. Hollenstein, M. Quack and M. Willeke, *Mol. Phys.*, 2006, **104**, 2719–2735.
125 S. Albert, K. K. Albert and M. Quack, *J. Mol. Struct.*, 2004, **695–696**, 385–394.
126 S. Albert and M. Quack, *J. Mol. Spectrosc.*, 2007, **243**, 280–291.
127 S. Albert, K. Keppler Albert, P. Lerch and M. Quack, *Faraday Discuss.*, 2011, **150**, 71–99.
128 S. Albert, P. Lerch and M. Quack, *ChemPhysChem*, 2013, **14**, 3204–3208.
129 S. Albert, P. Lerch, R. Prentner and M. Quack, *Angew. Chem., Int. Ed.*, 2013, **52**, 346–349.
130 S. Albert, K. Keppler and M. Quack, *Mol. Phys.*, 2015, **113**, 2267–2289.

131 J. K. G. Watson, *Vibrational Spectra and Structure*, Amsterdam, 1978, vol. 6, pp. 1–89.
132 H. M. Pickett, *J. Mol. Spectrosc.*, 1991, **148**, 371–377.
133 M. Stefko, M. D. Tzirakis, B. Breiten, M.-O. Ebert, O. Dumele, W. B. Schweizer, J.-P. Gisselbrecht, C. Boudon, M. T. Beels, I. Biaggio and F. Diederich, *Chem. – Eur. J.*, 2013, **19**, 12693–12704.
134 J. M. Matxain, J. M. Asua and F. Ruiperez, *Phys. Chem. Chem. Phys.*, 2016, **18**, 1758–1770.
135 R. Berger and M. Quack, *ChemPhysChem*, 2000, **1**, 57–60.